



University  
of Glasgow

Cresswell, A.J., Sanderson, D.C.W. and Murphy, S. (1999) *Improved NaI(Tl) and CsI(Tl) Detector Arrays for Environmental Airborne Gamma Spectrometry: Technical Progress Report*. Technical Report. Scottish Universities Research and Reactor Centre, East Kilbride, UK.

<http://eprints.gla.ac.uk/39217>

Deposited on: 20 December 2010



---

Scottish Universities Research & Reactor Centre

---

**Improved NaI(Tl) and CsI(Tl) Detector Arrays for  
Environmental Airborne Gamma Spectrometry**

**Technical Progress Report**

A.J. Cresswell, D.C.W. Sanderson, S. Murphy

December 1999

Work funded by the Engineering and Physical Sciences Research Council (EPSRC)  
Grant Number GR/M15842

## Summary

Airborne Gamma Spectrometry (AGS) is a well recognised method for mapping the distribution of natural and anthropogenic radionuclides in the environment using high-sensitivity  $\gamma$ -ray spectrometers mounted on aircraft. Such systems usually use large volume thallium doped sodium iodide (NaI(Tl)) spectrometers, conventionally consisting of a number of  $10 \times 10 \times 40$  cm ( $4000 \text{ cm}^3$ ) crystals each viewed by individual photomultiplier tubes. The energy resolution of such arrays is a significant factor affecting the sensitivity of the system to individual radionuclides. The higher energy  $\gamma$ -ray lines from the natural series are relatively well resolved and relatively easily measured, however, radionuclides of environmental relevance tend to have lower energy  $\gamma$ -ray lines which typically may be poorly resolved from other  $\gamma$ -rays with similar energies. In particular situations (such as early post-accident measurements of radioactive contamination) where complex mixtures of radionuclides exist these  $\gamma$ -rays may be impossible to resolve.

Methods of improving the response of such detectors have been investigated; specifically whether gating information and modifications to pulse analysis could improve the composite resolution of NaI(Tl) detector arrays and permit investigation of angular distribution and self-collimation effects, and whether the use of CsI(Tl) as an alternative scintillant could result in detector systems with improved resolution and efficiency compared to NaI(Tl) and how such a detector system might be produced.

To improve detector response a new second stage amplification system, a three stage shaping amplifier with a differentiation followed by two integrating stages, was developed. A prototype has considerably greater gain than the single amplifier previously used with improved resolution. Replacing the existing summing amplifier with a summing and shaping amplifier is straight forward and is expected to enhance the resolution of the array. A circuit to provide gating signals for individual NaI(Tl) crystals was also developed, and could be used to generate signals to identify which detector(s) register individual events, from which angular distribution and self-collimation information could be extracted from the array potentially yielding additional information on source distribution. Two methods of combining such gating systems with the three stage amplifier and an SAR ADC (evaluated separately) have been identified. Implementation of these developments would significantly enhance performance of the high volume NaI arrays in current use for AGS surveys.

It is known that CsI(Tl) produces more photons per MeV of incident radiation than NaI(Tl), with peak light emission at longer wavelengths where it is well matched to Si PIN photodiodes. Small CsI(Tl)-photodiode detectors have been used for  $\gamma$ -ray detection, and larger crystals for charge particle detection. The potential of using a large array of such detectors for AGS is explored.

A small commercially manufactured CsI(Tl)-photodiode detector consisting of a  $10 \times 10 \times 20$  mm CsI(Tl) crystal coupled to a  $10 \times 10$  mm photodiode with a hybrid preamplifier, was supplied for evaluation. This detector had a maximum resolution of 6.0% and full energy peak efficiency of 9.7% for  $^{137}\text{Cs}$   $\gamma$ -rays, depending on electronics and detector orientation, with a low energy threshold of approximately 100 keV. This has confirmed the improved spectral resolution of small CsI(Tl) crystals coupled to photodiodes. However crystals of this size may be considered undesirably inefficient for use in an airborne detector. If larger crystals can approach the performance of this crystal then a large detector array is more feasible.

A small 14×14×20 mm CsI(Tl) crystal attached to a 10×10 mm Si PIN photodiode was used to test other electronics systems. A Hamamatsu H4083 charge sensitive amplifier, a small hybrid chip designed to operate in conjunction with S3590 series photodiodes, had very low gain and poor noise characteristics, and is unsuitable for use with CsI(Tl)-photodiode detectors. A Canberra 970 preamplifier, a larger device consisting of discrete components mounted inside a shielded box, had good noise and gain characteristics, confirming that the material available in the UK, and diode mounting configurations were able to match the eV device, and that the 970 amplifier could be used for further performance tests.

Variations on the proposed electronics for recording spectra from individual NaI(Tl) detectors could be used with discrete preamplifiers such as the eV hybrid chip in an array of several CsI(Tl)-photodiode detectors. However, such a data logging system would become very complex with larger arrays, and would probably be limited to arrays of approximately 16 elements. The RAL-213 gamma camera IC is a 16 channel chip based on the SR1 chip, each channel consisting of a preamplifier, threshold comparator, variable shaping time shaping amplifier and peak hold circuit. Sixteen of these chips can be daisy-chained, sharing common busses, to allow 256 channels sharing a common ADC and sequence generating circuitry. The compact size and multichannel nature of these chips would be ideal for use with an array of a large number of individual CsI(Tl) crystals, if the performance of the chip is adequate.

A printed circuit board was developed to mount the RAL-213 chip, along with a 12-bit SAR ADC and an interface with an 8255 i/o card and PC to generate control pulses and collect the data. Within the time available it proved to be difficult to overcome practical problems getting this system to operate in a consistent and reproducible manner. Further work would be needed to overcome the practical problems associated with the use of this highly promising device.

To help determine optimal crystal dimensions, a series of CsI(Tl) crystals of a small range of sizes was obtained, and their spectral characteristics using a <sup>137</sup>Cs source and the Canberra preamplifier measured. There is a clear relationship between crystal dimensions and detector response; the gain and resolution degrades with increasing crystal size, and the full energy peak efficiency increases with the length of crystal material along the source-detector axis, reaching a maximum efficiency with about 8 cm of material along this axis. It has been shown that CsI(Tl) crystals larger than a few cm<sup>3</sup> can still produce improved spectral resolution compared to NaI(Tl), although further work is still required to determine optimal crystal geometries.

These crystals, when mounted, have a pink tint, which is expected to effect the transmission of scintillation luminescence within the crystals, and thus explain the low light collection efficiency of the larger crystals. ICPMS analysis conducted on samples of CsI(Tl) has shown that both clear and coloured crystals contain Ni impurities at between 130 and 200 ppm, and presumably Fe is also present although the analysis is insensitive to it. It is possible that the pink colour is due to variation in oxidation state or coordination site of these contaminants. It was also noted that the pink crystals had slightly higher Ni levels, and reduced Tl levels, implying that the Ni may inhibit Tl uptake in the crystal.

Three generations of Monte Carlo codes have been previously developed for modelling the response of NaI(Tl) AGS detectors, which, to fully simulate spectra, require experimentally measured spectral characteristics, and so cannot be used to investigate the effects of crystal size on the detector resolution. Even without this prior knowledge these codes can still effectively

model effects such as full energy peak efficiencies, peak to Compton ratios and self-collimation effects. For crystals with known characteristics, the response of a large array to different sources or source geometries can be more fully simulated. Other codes, such as GEANT, should be capable of modelling the response of individual crystals more completely but are less suited to simulating airborne geometries due to the large source to detector distances.

The codes have been modified to simulate a CsI(Tl) detector by replacing NaI(Tl) scattering and absorption terms with corresponding CsI(Tl) terms, and used to simulate spectra from a 10×10×20 mm crystal in the same geometries as the eV detector previously tested, generating reasonably accurate simulated spectra for close-coupled geometries. The codes, for both CsI(Tl) and NaI(Tl), were also modified to produce interaction lists consisting of the position and deposited energy for each interaction in the detector volume. This data can be used to investigate the effect of detector segmentation, help determine optimal dimensions for individual elements of a large array, and investigate angular correlation and self-collimation effects. The results of these simulations slightly over estimate the full energy peak efficiency for NaI(Tl), but produce the physically realistic results that full energy peak efficiency is greater for CsI(Tl) than NaI(Tl) and that higher energy  $\gamma$ -rays have lower efficiencies. The distance between interactions is somewhat surprising given the data from the comparison between crystals of different dimensions. Spectra for particular small volumes within the crystal, corresponding to elements in an array, may also be produced; although this has yet to be done.

To investigate whether self-collimation effects within an array can provide information on source burial these codes, for CsI(Tl) and NaI(Tl), were also modified to incorporate source burial. The results of these modifications, for an otherwise extensively validated code, produced spectra with a non-physically realistic lack of scatter. Because of this effect, and the surprisingly dispersed spatial distribution of energy deposition noted above, the results should be treated with caution at this stage. More work is needed to validate these codes further and to compare them with other MC simulations of sources in laboratory geometries, and with experimental results from a small array of detectors.

It has been shown that it is possible to improve on the spatial response and data acquisition systems currently used in AGS through modifications to the electronics and computational methods used with existing NaI(Tl) detectors. It has also been shown that the use of CsI(Tl) crystals coupled to Si PIN photodiodes can generate data with greater spectral resolution than NaI(Tl), although only for relatively small crystals. Although there is still considerable work to be done to produce a large volume array of CsI(Tl) detectors for use in AGS, some of the means by which such an array could be constructed and operated have been identified. These improvements should enhance the ability of AGS to quantify the activity of radioisotopes in the environment through reduced spectral interferences and better knowledge of source distribution.

## Contents

1. Introduction .....	1
1.1 Properties of Scintillators.....	1
1.2 Properties of NaI(Tl) and CsI(Tl).....	2
2. Experimental Investigations of Improve NaI(Tl) and CsI(Tl) Detector Systems.....	5
2.1 Electronics for Possible Improved NaI(Tl) Systems.....	5
2.2 Evaluation of CsI(Tl)-photodiode Detector Systems.....	10
2.3 Investigation of Crystal Dimensions.....	18
3. Monte Carlo Simulation of NaI(Tl) and CsI(Tl) Detectors.....	20
3.1 Simulation of eV Detector Response.....	20
3.2 Analysis of Deposition Patterns Within Crystals.....	22
3.3 Analysis of Deposition Lists for Source Burial Analysis.....	23
4. Discussion and Conclusions.....	25
Acknowledgements.....	29
References.....	30

## 1. Introduction.

Airborne Gamma Spectrometry (AGS) is a well recognised method for mapping the distribution of natural and anthropogenic radionuclides in the environment using high-sensitivity  $\gamma$ -ray spectrometers mounted on aircraft [1-5]. Several teams within Europe [6] and elsewhere have gained considerable experience in using such equipment. The team based at SURRC has used the technique in some 20 different surveys since 1988; including nuclear site base line surveys [7-13], epidemiological studies of links between environmental radiation and cancers [14], surveys of Chernobyl fallout [15-19] and Sellafield discharges [7-9,15,18] and nuclear emergency response preparedness exercises. Currently, such systems usually use large volume thallium doped sodium iodide (NaI(Tl)) spectrometers, conventionally consisting of a number of  $10 \times 10 \times 40$  cm ( $4000 \text{ cm}^3$ ) crystals each viewed by individual photomultiplier tubes. In fixed wing aircraft arrays of 48 or 64 litres are commonly used, in helicopters 16 or 32 litre arrays are more commonly used. Detection limits of  $1\text{-}2 \text{ kBq m}^{-2}$  are possible for fission products with well resolved high energy  $\gamma$ -rays using such systems.

Individual 4 litre NaI(Tl) crystals have energy resolutions typically of 7.5-8.5% for the 662 keV  $^{137}\text{Cs}$   $\gamma$ -ray, with summed arrays this resolution is degraded to 9-10% with 4 crystals. The energy resolution of such arrays is a significant factor affecting the sensitivity of the system to individual radionuclides. The higher energy  $\gamma$ -ray lines from the natural series (eg: 1462 keV  $^{40}\text{K}$ , 1764 keV  $^{214}\text{Bi}$  and 2614 keV  $^{208}\text{Tl}$ ) are relatively well resolved and relatively easily measured. However, radionuclides of environmental relevance tend to have lower energy  $\gamma$ -ray lines (eg: 60 keV  $^{241}\text{Am}$ , 365 keV  $^{131}\text{I}$  and 662 keV  $^{137}\text{Cs}$ ). These  $\gamma$ -rays typically may be poorly resolved from other  $\gamma$ -rays with similar energies, in particular in situations (such as early post-accident measurements of radioactive contamination) where there exists complex mixtures of radionuclides these  $\gamma$ -rays may be impossible to resolve [20].

Several approaches to improve the ability of AGS systems to measure the distribution of such isotopes in the environment. These approaches include the use of combined systems incorporating NaI(Tl) and high resolution Ge semiconductor detectors [20-22] and several spectral analysis methods [23-24]. Another potential approach is to develop a detector system which has the high efficiency of NaI(Tl) with improved spectral resolution, either as a result of improvements to existing NaI(Tl) systems or by use of an alternative scintillant. Both approaches are explored in this project; with an investigation into the possibility of developing a detector system based on thallium doped caesium iodide (CsI(Tl)) scintillators coupled to silicon photodiodes, and the development of a more sophisticated pulse analysis system for NaI(Tl) detectors producing improved spectral resolution and gating circuitry to provide more flexible data logging that may allow angular distribution and self-collimation effects within an array to be utilised; such effects may provide additional source distribution, such as source burial, data that would enable more accurate calibration of AGS equipment.

### 1.1 Properties of Scintillators.

Scintillating materials are routinely used for the detection of radiation. When  $\gamma$ -rays or other energetic radiations interact with such materials they deposit energy at particular locations within the material, which is released as a large number of photons of infra-red or visible light. If the material is sufficiently transparent these photons can be transmitted to the surface, where they

	BGO	CsI (Tl)	NaI(Tl)	Typical plastic
Density (g cm <sup>-3</sup> )	7.13	4.51	3.7	1.03
Wavelength of maximum emission (nm)	505	540	415	423
Photon yield (1000 photons/MeV)	5-15	45	40	10
Refractive index	2.15	1.8	1.85	1.58
Decay time (ns)	300	900	230	2
Afterglow (% after 3 ms)	0.05	4.5	5	

**Table 1.1:** Selected properties of Bismuth germanate (BGO), thallium doped caesium iodide (CsI(Tl)), thallium doped sodium iodide (NaI(Tl)) and a typical plastic scintillator.

can be detected. The number of photons produced is proportional to the energy deposited by the radiation in the material, and, providing there is no significant difference in photon loss for interactions in different parts of the crystal, this proportionality is retained for the number of photons detected.

Several scintillating materials have been used for radiation detection. These include plastics, bismuth germanate (BGO) and alkali halides (NaI and CsI) often containing dopants which alter the light emission characteristics. The differing mechanical and optical properties of these materials determine their response to radiation, and hence the uses to which these materials are put. Table 1.1 lists selected relevant properties for some of these materials [25,26]. Plastic scintillators are cheap materials with very short decay times resulting in narrow pulses, however their low density means large volumes are required and low light output limits the energy resolution; they are often used for the detection of neutrons or beta-particles which are absorbed in relatively small amounts of material. Gamma-ray detectors usually utilise inorganic scintillators due to their higher density and larger Z values. The very high density of BGO would allow small volume detectors, but the low light output severely restricts spectral resolution, and so is usually used in situations where low volume is required but spectral resolution is not important. In situations where both detection efficiency and spectral resolution are important NaI(Tl) and CsI(Tl) are good compromises.

## 1.2 The Properties of NaI(Tl) and CsI(Tl).

Traditionally, NaI(Tl) has been the material of choice for most applications, primarily due to the fact that the luminescence emission is well matched to bi-alkali photomultipliers. Recently, however, the use of CsI(Tl) has become more common. A major factor determining the resolution of scintillators is the number of photons detected, which have a Poisson distribution.



The relative variation in the number of detected photons is reduced with greater number of photons detected, and hence the resolution from detectors in which greater numbers of photons are captured is improved. Compared to NaI(Tl), CsI(Tl) produces a greater number of photons per MeV of the incident  $\gamma$ -ray, and with a greater number of photons produced CsI(Tl) should have better resolution than NaI(Tl). However, the average wavelength of the photons produced in the crystal is longer than that for NaI(Tl) and is not as well matched to traditional photomultipliers resulting in less photons being captured and poorer resolution. The photons produced by CsI(Tl) are, however, well matched to silicon PIN photodiodes; the combination of CsI(Tl) and photodiodes should be able to capture a greater number of photons resulting in improved resolution.

Small volume CsI(Tl) crystals coupled to PIN diodes have been used in detectors for  $\gamma$ -ray telescopes (such as the INTEGRAL project [27]), radiation monitoring in the nuclear industry [28,29], calorimeters and other particle physics detectors [30-34], neutron-activation analysis [35] and medical imaging [36]. In most of these cases relatively small crystals, usually 1-2 cm<sup>3</sup>, have been investigated for  $\gamma$ -ray detection, although larger crystals have been used for the detection of charged particles.

To generate usable electrical signals from Si PIN diodes a charge sensitive preamplifier is required. The diode is a capacitive device with very high impedance, the output of which is a weak charge pulse. The charge sensitive preamplifier has a high impedance front end operational amplifier mode integrator with feedback capacitance which integrate the weak charge pulses, converting them into voltage pulses. The output stage is a low impedance buffer to drive an external second stage amplifier, often connected by a long cable [25,37].

The electronic noise, in root mean squared number of electrons, generated in the photodiode and subsequent amplification stages is related to the leakage current ( $I_d$ ) and diode capacitance ( $C$ ), according to the approximate relationship [28,38];

$$\sigma(\text{rms } e^-) = aI_d\tau + \frac{bC^2}{\tau}$$

where  $a$  and  $b$  are constants, and  $\tau$  is shaping time for the amplification network. The capacitance of the diode is related to the diode surface area ( $A$ ) and depth of the depletion layer ( $d$ );

$$C = \epsilon A/d$$

The dark current is produced as a result of surface and bulk volume effects in the silicon, and so is proportional to the detector volume and surface area. Increasing the bias voltage increases the depth of the depletion layer, and hence decreases the capacitance, and also increases the dark current.

The use of CsI(Tl) PIN diode detectors in a large array could, therefore, result in the production of a detector system with improved energy resolution compared to the conventional NaI(Tl) detector arrays used in AGS systems while maintaining the high efficiency of scintillator systems. In addition, the use of PIN diodes rather than photomultiplier tubes would eliminate the need for high voltage supplies and reduce the weight and bulk of the detectors. PIN diodes are typically more stable than photomultipliers, and so are less prone to gain drift which can be problematic in NaI(Tl) systems.

The need to minimize noise in the detector system means that the detector would need to be composed of a large number of small individual crystals, each with a photodiode and preamplifier. There is a potential benefit from using an array of a large number of crystals. The crystals towards the centre of the array are collimated by the outer crystals of the array, resulting in  $\gamma$ -rays from the side of the array being preferentially detected in the outer crystals. This self-collimation effect may result in the generation of additional information on the distribution of  $\gamma$ -emitting radioisotopes in the environment, such as source burial depth profiles. The use of self-collimating BGO detectors for locating point sources has also been investigated [39]. Such information may also be available by comparison between the inner and outer pairs of detectors in a conventional NaI(Tl) detector pack of four crystals. The electronic systems required to collect the data from an array of several crystals, or to exploit self-collimation effects within an array, would need to be more sophisticated than the electronics currently used in NaI(Tl) arrays.

## **2. Experimental Investigations of Improved NaI(Tl) and CsI(Tl) Detector Systems.**

Current Airborne Gamma Spectrometry (AGS) systems use large volume NaI(Tl) crystals coupled to photomultiplier tubes as the principal detector. These detectors comprise four, or for use in fixed wing aircraft sometimes more, individual 10×10×40 cm crystals with the signals from the individual crystals combined to give a voltage proportional to the total energy deposited in the entire array. Conventionally the electronics used in such systems are fairly simple, usually a single amplifier to sum the outputs of all the detectors in the array. An Ortec 916 ACE card, or similar, is usually used to record spectra from such a system; this board, mounted on a PC expansion slot, has integral processing components that run the spectrometry system, including histogramming spectra and monitoring dead time, without utilising processing resources of the PC. The use of such a data logging system allows the PC to store data to hard drive, monitor other equipment (such as GPS systems and radar-altimeters) and display real time data without introducing detector dead time.

This project has looked at means of improving the performance of such detector systems, either through use of an alternative scintillant or improved electronics systems. It is known that CsI(Tl) when coupled to Si PIN photodiodes has improved spectral resolution compared to NaI(Tl), at least for small crystals, and has a greater  $\gamma$ -ray absorption efficiency. Whether this enhanced performance is repeatable with larger crystals, and some questions relating to electronic requirements for a large array of relatively small crystals are addressed here.

### **2.1 Electronics for Possible Improved NaI(Tl) Systems.**

During the period of this project an experiment in laser-induced nuclear physics was conducted [40], for which a means of measuring the activity of weak positron sources was required. For this a pair of large volume NaI(Tl) detectors, with the source placed between them, was used to detect coincident pairs of 511 keV annihilation  $\gamma$ -rays. A circuit was developed produce gating signals when the two detectors simultaneously register  $\gamma$ -ray interactions, using comparators on the signals from the detector preamplifiers and a monostable unit to generate logic signals when the detector output exceeded a lower threshold. An AND gate generated a gating signal if both detectors produced a signal in excess of the threshold. By setting the threshold sufficiently high (approximately 450 keV) and using the spectrometric information recorded by an Ortec 916 ACE card it was possible to measure the activity of weak positron sources, especially when the detectors were placed in a lead shield to produce a low background environment. Figure 2.1 shows a schematic of this circuit, it was originally intended that this circuit use a second comparator to veto the gate if the input exceeded an upper threshold, however this did not work using this simple circuit due to the rise time of the preamplifier output.

To enable two pairs of NaI(Tl) detectors to be used for coincidence counting, a new second stage amplifier for the four element NaI(Tl) detector was produced. This was a minor modification on the single summing amplifier used for airborne measurements with a four detector pack. Instead of a single amplifier two amplifiers were used, each summing and amplifying the output of a pair of detectors.

This modified summing amplifier would allow spectra for the inner and outer pairs of crystals in the 16 litre pack to be recorded separately using two ACE cards, although this has yet to be done.

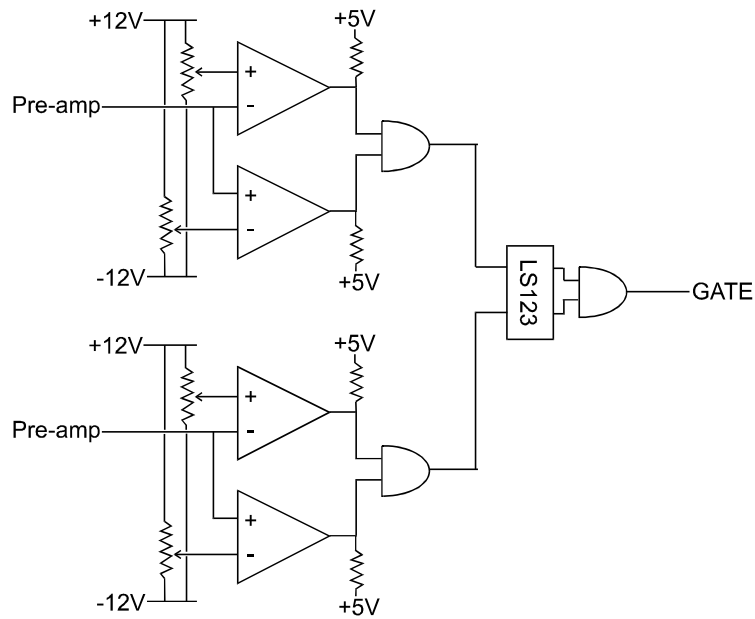


**Figure 2.1:** Schematic of the coincidence circuit

An experiment can be undertaken in which a series of medium density fibre boards, which have similar absorption properties to soil, and perspex sheets (which simulate the air path) are placed between a source and the detector. Such experiments have been conducted to investigate the response of the full NaI(Tl) detector array to buried sources [41], enabling the effects of scattering in the soil and the air path to be studied in controlled laboratory geometries. Experiments of this kind have not been conducted to investigate the response of a self-collimated detector setup, and the geometry of such an arrangement may not be suitable given that the source is mostly directly below the detector. Minor modifications to the coincidence circuit would enable the production of signals to identify which crystals had fired for each event, although the data collection and recording methodology would have to be modified to make full use of this information.

One option for revising the data collection to make use of the gating information is to use an ADC chip to convert the analogue signals to digital form, and then store the information in separate spectra depending on the gating signals. A suitable ADC, a Burr-Brown ADS7831 12-bit SAR chip [42], had been purchased for use with a gamma camera IC evaluated during studies of CsI(Tl)-photodiode detectors conducted in parallel with these modifications to NaI(Tl) detector electronics. A printed circuit board had been produced to mount this chip and the ADC, the possibility of using this ADC to record spectra from NaI(Tl) detectors was investigated by using the output from the summing amplifier in the NaI(Tl) detector pack, with only one crystal used, as the analogue input to the ADC. A comparator on the preamplifier output of the crystal, similar to that used in the coincidence circuit, was used to generate the convert signal to start conversion.

Figure 2.2 shows a spectrum recorded over an arbitrary short integration time from a  $^{137}\text{Cs}$  source using the ADS7831 ADC chip. This clearly shows that the ADC was operating correctly, and that it is possible to use such a system to record spectra. It is also evident that this spectrum has poor resolution and a distinctly non-linear gain, the 662 keV  $^{137}\text{Cs}$   $\gamma$ -ray peak was placed approximately in channel 662, yet the 1462 keV  $^{40}\text{K}$   $\gamma$ -ray peak is approximately in channel 1050. The internal

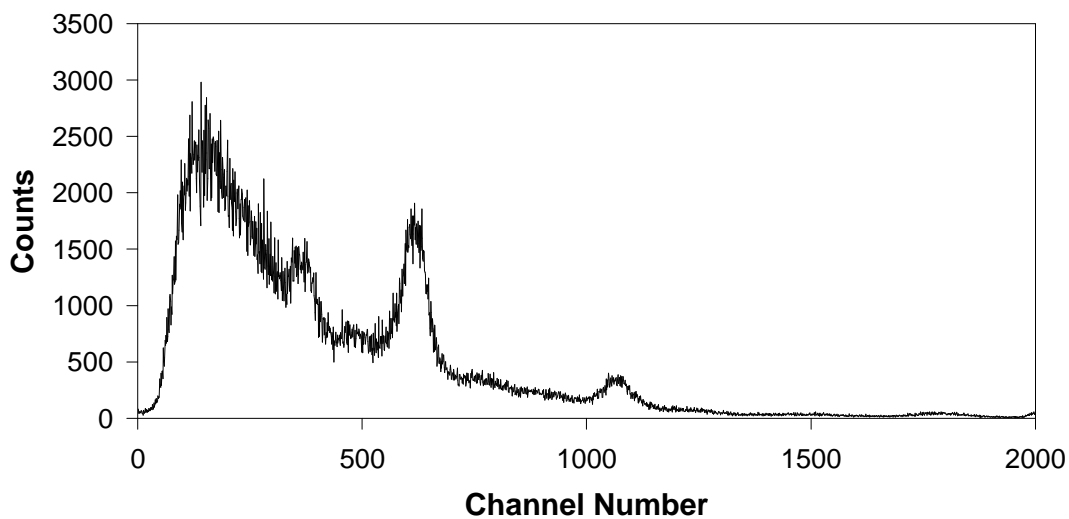


**Figure 2.2:** Spectrum recorded using ADS7831 ADC with analogue input produced by a single NaI(Tl) crystal.

sample and hold circuit within the ADS7831 holds the voltage at the level it was at when conversion started even if the input signal reaches a higher level later. The poor resolution and non-linearity in the spectrum is due to the variation in rise time for the amplifier outputs for different energy events resulting in the conversion not always starting at the top of the amplifier pulse. This effect is avoided with the RAL-213 chip because it incorporates a sample and hold circuit so a constant voltage level is presented to the ADC. Any other input to this ADC would require a constant rise time, with well timed conversion signals, or a sample and hold circuit to present a similar constant voltage signal.

A new second stage amplification system, consisting of a three stage shaping amplifier, was developed to improve the response of NaI(Tl) detector systems. It is expected that better pulse shaping would reduce the problems associated with the variation in rise time when using the ADS7831 chip to log spectra, and could also improve the spectral resolution for the current system using ACE cards to record spectra. Figure 2.3 shows a schematic of this amplifier, a prototype of which was produced using a single TL084CN quad op-amp with the values of the resistors and capacitors determined empirically. The amplifier consists of a differentiation stage, which produces a bi-polar pulse with the cross-over point almost independent of the preamplifier pulse height, followed by two integration stages which result in a near Gaussian shaped positive going pulse with a rise time which is much less dependent on the peak height than the simpler summing amplifier.

The prototype shaping amplifier was built on VERO board, and was not placed within a shielded container, and as such there would be more electronic noise compared to an amplifier built on a PCB and shielded. Nevertheless, when compared to the single stage summing amplifier there was a marked improvement in spectral response. The two amplifiers were used with a single NaI(Tl) detector and an Ortec 916 ACE card to record spectra from a  $^{137}\text{Cs}$  source, which are shown in figure 2.4. It is noted that the gain of the three stage shaping amplifier is considerably greater than the single summing amplifier (with the  $^{137}\text{Cs}$  peak in channel 800 rather than 310), but the resolution is improved (8.8% FWHM rather than 9.1%). There is a

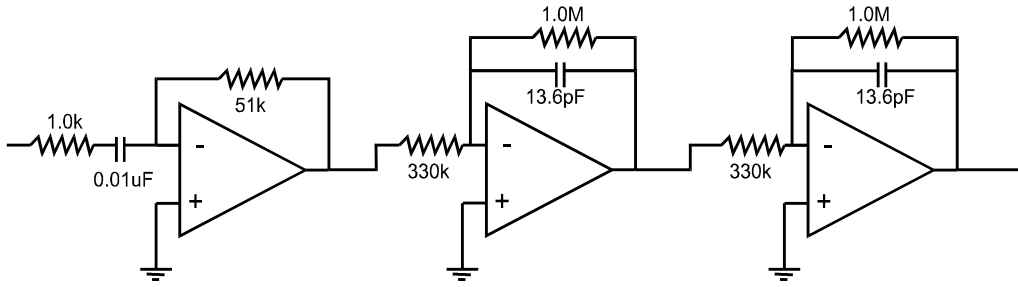


**Figure 2.3:** Schematic of the three stage shaping amplifier

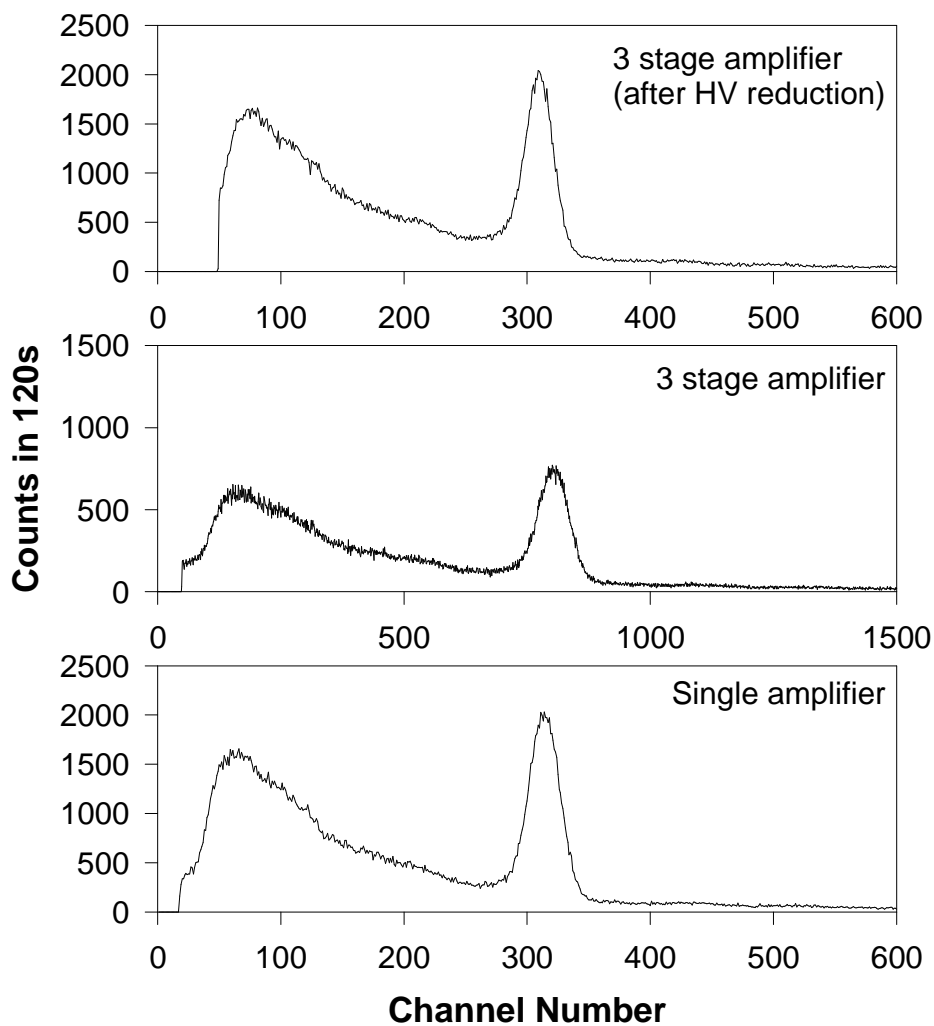


**Figure 2.4:** Spectra recorded from a  $^{137}\text{Cs}$  source by a single NaI(Tl) crystal using a single stage amplifier or the three stage shaping amplifier before and after the HV was reduced.

distinct upper threshold in the spectrum for the three stage amplifier, with a single channel spike, which is probably due to one of the amplifiers producing an output in excess of its 12 V maximum level. Reducing the HV to put the  $^{137}\text{Cs}$  peak in channel 310 results in this amplifier effect being significantly above 3 MeV, with a FWHM of the  $^{137}\text{Cs}$  peak of 8.2%. It has been shown that more sophisticated amplification can improve the resolution of NaI(Tl) detectors, although reducing the HV further, the HV is usually adjusted until the  $^{137}\text{Cs}$  peak is in channel 112, may degrade the signal to noise ratio of the photomultiplier tube in which case lower gain in the amplifier would be needed. To replace the existing summing amplifier with a summing and shaping amplifier would involve using four 1.0 k $\Omega$  input resistors for each of the four input signals, with these lines being combined prior to the 0.01  $\mu\text{F}$  capacitor. This would be a simple modification, and is expected to result in an improvement in the spectral resolution of the summed array.

Two possible methods of developing an advanced signal processing system capable of utilising any self-collimation effects in the NaI(Tl) detector pack using this three stage shaping amplifier and the ADS7831 ADC have been considered. Both of these involve a comparator on each preamplifier output, similar to the coincidence unit, to identify which detector(s) have recorded a  $\gamma$ -ray interaction and to trigger conversion (either directly or via a PC interface). Both systems would register individual events, which the computer could add to one or more spectra depending on which detectors fired. Alternatively, the data could be recorded on an event-by-event basis for later processing. In both cases the computer resources required to run such a system may require a computer dedicated to this task; this is not fundamentally different from the current system in which processors on the 916 ACE card handle all the histogramming of the spectra, which are then read by the PC at the end of each data logging interval. Neither method presented here includes any means of measuring detector dead time, although it may be possible to add such a feature at a later date. Figure 2.5 gives schematics of these two methods.

The first, and simplest, of these methods uses one shaping amplifier to produce a summed output which is then used as the input for the ADC, the timing of the convert pulse generated by the comparator must be precise for correct conversion unless a sample and hold circuit is included. The computer records the summed spectrum, but could only record spectra for individual detectors if a single detector fires for that event. This approach would work if the number of events involving multiple detectors was small, however it is expected that many of the incident  $\gamma$ -rays would deposit energy in more than one detector, especially at higher energies and where the first point of interaction is near the boundary between two detectors.

The second method uses five shaping amplifiers for each individual channel and the summed output with an analogue multiplexer to process one signal at a time. Sample and hold circuits are required to maintain voltage levels at the multiplexer input until conversion, the comparator signals are used to generate the hold signal as well as identify the detector(s) that registered each event. This circuit can record spectra for each detector, or spectra from any combination of detectors depending on the program used. It would work equally well for events involving one or more than one detector.

Within the time scale of this project it has not been possible to test any components of these models, except the shaping amplifier and ADC, or prototype either of these models of enhanced NaI(Tl) detector electronics. It has yet to be determined whether a system less well suited to multi-detector interactions, ie: the first model, would suffice or whether the more

complex circuit would be needed.

## 2.2 Evaluation of CsI(Tl)-photodiode Detector Systems.

It is possible to purchase small CsI(Tl)-photodiode detector systems from commercial companies consisting of crystal, diode and preamplifier; one such detector was acquired for evaluation. However, such detectors are only available commercially in relatively small sizes, although if sufficient numbers were required larger detectors could presumably be manufactured. So, in addition to this small detector components necessary for the production of custom detectors were also evaluated, specifically photodiodes and preamplifiers and a range of different crystal geometries. Evaluation of such components should help clarify the requirements for crystals and electronics for use in a large array of CsI(Tl)-photodiode detectors.

A small CsI(Tl)-photodiode detector produced by eV Products was supplied on loan by Gresham Scientific for evaluation purposes. This consisted of a 10×10×20 mm CsI(Tl) crystal coupled to a 10×10 mm Hamamatsu Si photodiode with an eV hybrid preamplifier. The test spectrum supplied [43] with the detector gave a FWHM of 5.9% for the 662 keV <sup>137</sup>Cs peak, using an amplifier with a 6 μs shaping time and a 40 V bias voltage. The geometry used to derive this spectrum was not supplied. The response of this detector was tested using several NIM based amplifiers, with different shaping times, using a <sup>137</sup>Cs source. The optimum amplifier and shaping time was then used to test the detector response to a variety of γ-ray sources, and two detector orientations.

Initial testing was conducted with a poor quality connection for the preamplifier output lead, and as a result some additional electronic noise was introduced to the system. Two Ortec amplifiers, models 570 and 571, were used with 3 different shaping times keeping the gain on each amplifier constant after initially setting the gains of the two amplifiers to approximately the same value. A <sup>137</sup>Cs source was placed on the bench approximately 3 cm from the detector, and a reverse bias of 40 V applied to the diode. An Ortec 916 ACE card, without altering the low limit of detection, and Ortec software were used to record spectra for each system, and the dead time and channel position and FWHM for the 662 keV peak noted; these values are given in table 2.1. This shows that increasing the shaping time results in increased gain and dead time, and that the optimum combination of resolution and dead time was obtained using a 570

**Figure 2.5:** Two possible circuits for improved signal processing for NaI(Tl) detectors.

amplifier with a 6 μs shaping time. This is consistent with previous work which has also shown

Shaping time (μs)	570 amplifier			571 amplifier		
	Dead time	<sup>137</sup> Cs channel	FWHM	Dead time	<sup>137</sup> Cs channel	FWHM
3	1.2%	93.48	7.20%	0.8%	95.69	7.13%
6	3.3%	107.17	7.02%	1.0%	118.92	7.13%
10	5.1%	116.71	7.42%	1.2%	133.30	7.00%

**Table 2.1:** The dead time, channel number and FWHM of the 662 keV <sup>137</sup>Cs peak for the Ortec 570 and 571 amplifiers.



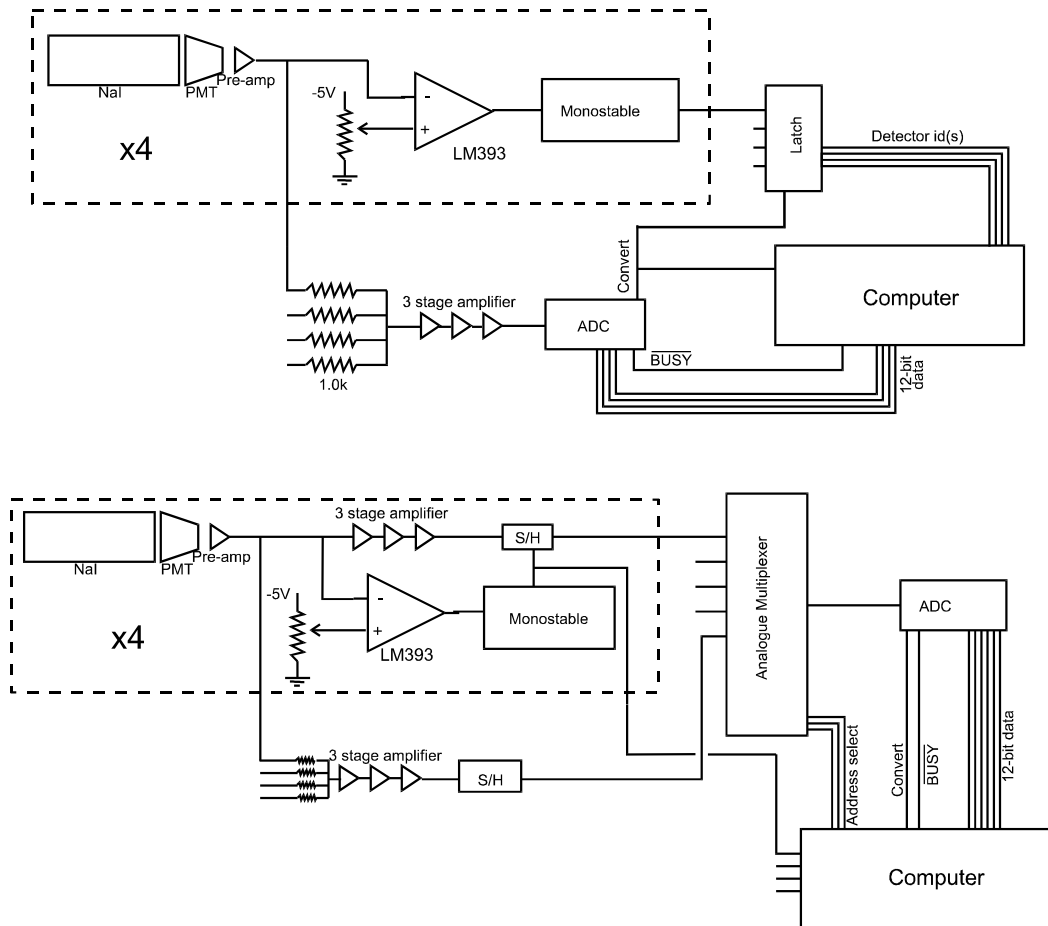


**Figure 2.5:** Two possible circuits for improved signal processing for NaI(Tl) detectors.

that the resolution of CsI(Tl)-photodiode detectors is best for shaping times of about  $6 \mu\text{s}$  [34].

After an improved connector had been fitted to the preamplifier output the amplifiers were tested again using a  $6 \mu\text{s}$  shaping time. Two 570 amplifiers were tested, one had a dead time of 3.1% and a FWHM of 6.35% the other a dead time of 7.4% and a FWHM of 6.01%, the 571 amplifier had a dead time of 0.8% and a FWHM of 6.68%. The dead time was dependent mainly on the low energy noise from the diode, and could be altered by changing the ADC threshold. One of the 570 amplifiers reproduced the resolution of the test spectrum supplied with the detector, and this amplifier was used for all further testing. The 571 amplifier should be better than the 570 amplifiers. The pole-zero of these amplifiers was not adjusted, although such adjustments could slightly improve the detector resolution. Other amplifiers were also tested, but produced worse performances.

The detector was placed 40 cm above a point source placed on a concrete plinth, and a series of spectra for  $^{137}\text{Cs}$ ,  $^{60}\text{Co}$  and  $^{133}\text{Ba}$  sources and natural backgrounds were recorded, and are shown in figure 2.6. The detector was oriented such that the long axis was vertical, and the ADC lower threshold adjusted to just above the low energy noise (channel 16, corresponding to an energy of approximately 100 keV). The resolution for this system was 6.2% for the 662 keV  $^{137}\text{Cs}$   $\gamma$ -ray, falling to 3.7% for the 1462 keV  $^{40}\text{K}$   $\gamma$ -ray and 2.0% for the 2615 keV  $^{208}\text{Tl}$   $\gamma$ -ray.

The full energy peak efficiency of this detector for the 662 keV  $\gamma$ -ray was 9.7%, after accounting for the solid angle.

Similar spectra were recorded with the detector placed such that the long axis was horizontal, with all other factors unaltered. These spectra are shown in figure 2.7. For the detector in this orientation the resolution for the 662 keV peak was 6.2%, for the 1462 keV 3.4% and for the 2615 keV 1.7%, with a full energy peak efficiency for the 662 keV  $\gamma$ -ray of 5.3%. Compared to the vertical orientation the horizontal orientation has improved resolution, especially at higher energies, but reduced full energy peak efficiency.

Evaluation of this unit has demonstrated that small CsI(Tl) crystals coupled to photodiodes with compact hybrid preamplifiers can produce signals with improved spectral resolution compared to NaI(Tl) detector systems. However, crystals of this size may be considered undesirably inefficient for use in an airborne detector, with a significant proportion of scattered events being lost to its edges. The full-energy efficiency within a large array will be significantly enhanced compared to a single crystal, but a significant proportion of these events are expected to arise from partial deposition in a number of individual crystals. In addition, to create an array of comparable efficiency to the NaI(Tl) systems currently used several thousand crystals of this size would be required. If larger crystals can approach the spectral resolution of this crystal then a large detector array is more feasible.

To evaluate electronic systems for use with CsI(Tl)-photodiode detectors, a small 14×14×20 mm CsI(Tl) crystal attached to a Hamamatsu S3590-08 10×10 mm Si PIN photodiode was prepared by Hilger Crystals. This was mounted in a die-cast box, which was earthed to reduce noise due to external sources. This was then used for testing a number of amplification systems.

Two discrete preamplifiers were evaluated; a Hamamatsu H4083 charge sensitive amplifier and a Canberra 970 preamplifier borrowed from Glasgow University Physics Department. The Hamamatsu preamplifier [37] is a small hybrid chip designed to operate in conjunction with Hamamatsu Si PIN photodiodes such as the S3590 series, onto which it may be directly soldered to reduce input capacitance, and requires an external load resistor to be placed between the diode and bias voltage supply. This unit is primarily intended for direct conversion of high energy radiation within the photodiode rather than measuring scintillation interactions. The Canberra preamplifier is an older unit, consisting of discrete components mounted inside a shielded box including the load resistor. In both cases the better Ortec 570 amplifier was used for final stage amplification, and spectra were recorded using an Ortec 916 ACE card.

The S3590-08 photodiode [37] is made from 300  $\mu\text{m}$  thick Si, and has a stated maximum reverse voltage of 100 V. At a bias of 70 V a typical dark current of 2 nA and terminal capacitance of 40 pF is quoted. It was assumed that 70 V is the optimum reverse bias for this diode, but a short experiment in which spectra from a  $^{137}\text{Cs}$  source were recorded for a range of reverse bias voltages using the Canberra amplifier was conducted to confirm this. Table 2.2 lists the resolution for the  $^{137}\text{Cs}$  662 keV peak at a range of voltages between 20 and 100 V; the spectrum with 70 V reverse bias was recorded last, and the surprisingly poor resolution may mean the diode was adversely affected by operating it at the stated maximum voltage. This quick test confirms that 70 V is the optimum operating reverse bias voltage, and this bias was used for all subsequent work using this diode.

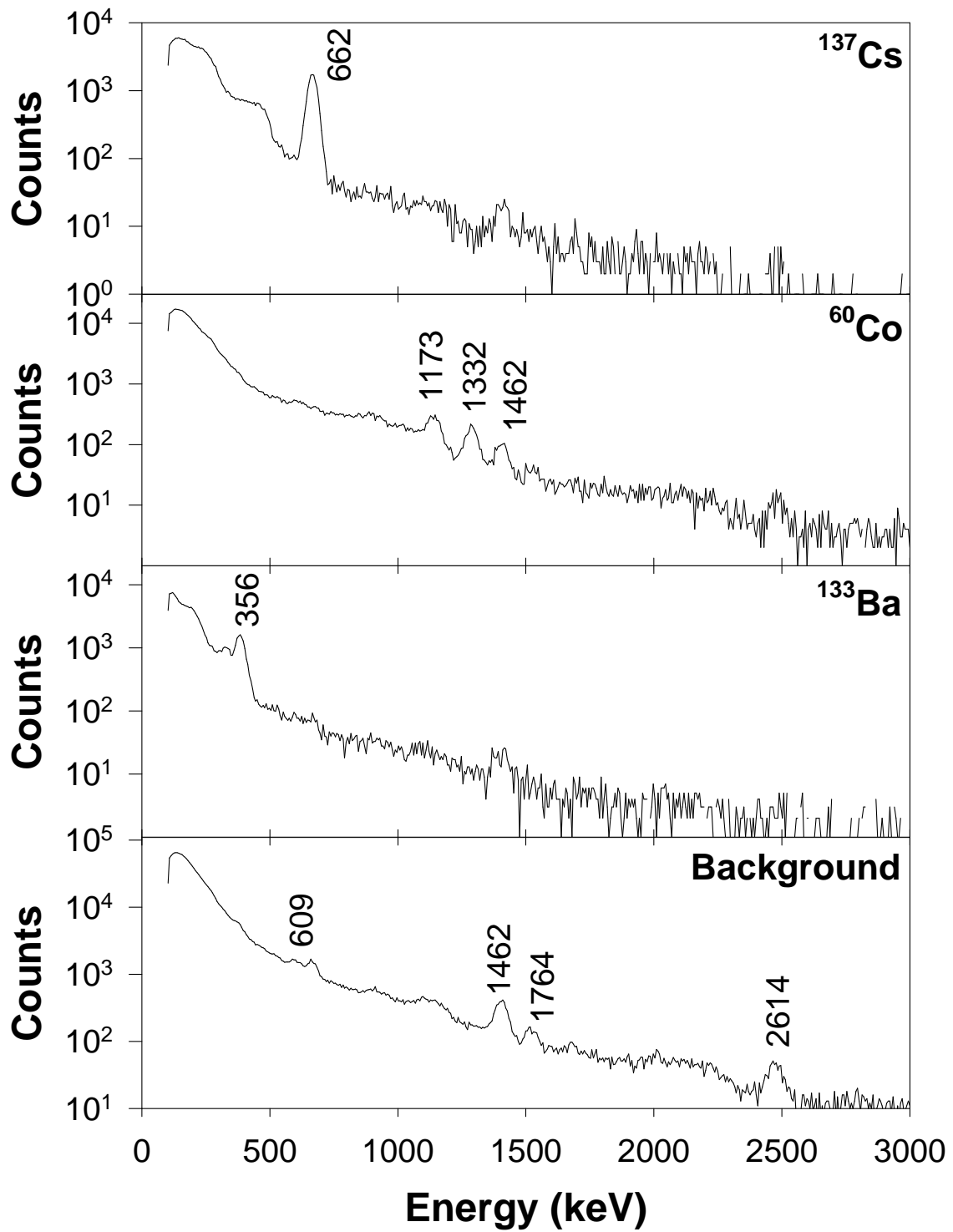


**Figure 2.6:** Spectra recorded from  $^{137}\text{Cs}$  (10000s livetime),  $^{60}\text{Co}$  (50000s livetime),  $^{133}\text{Ba}$  (10000s livetime) sources and laboratory background (200000s livetime) for the eV detector oriented vertically.

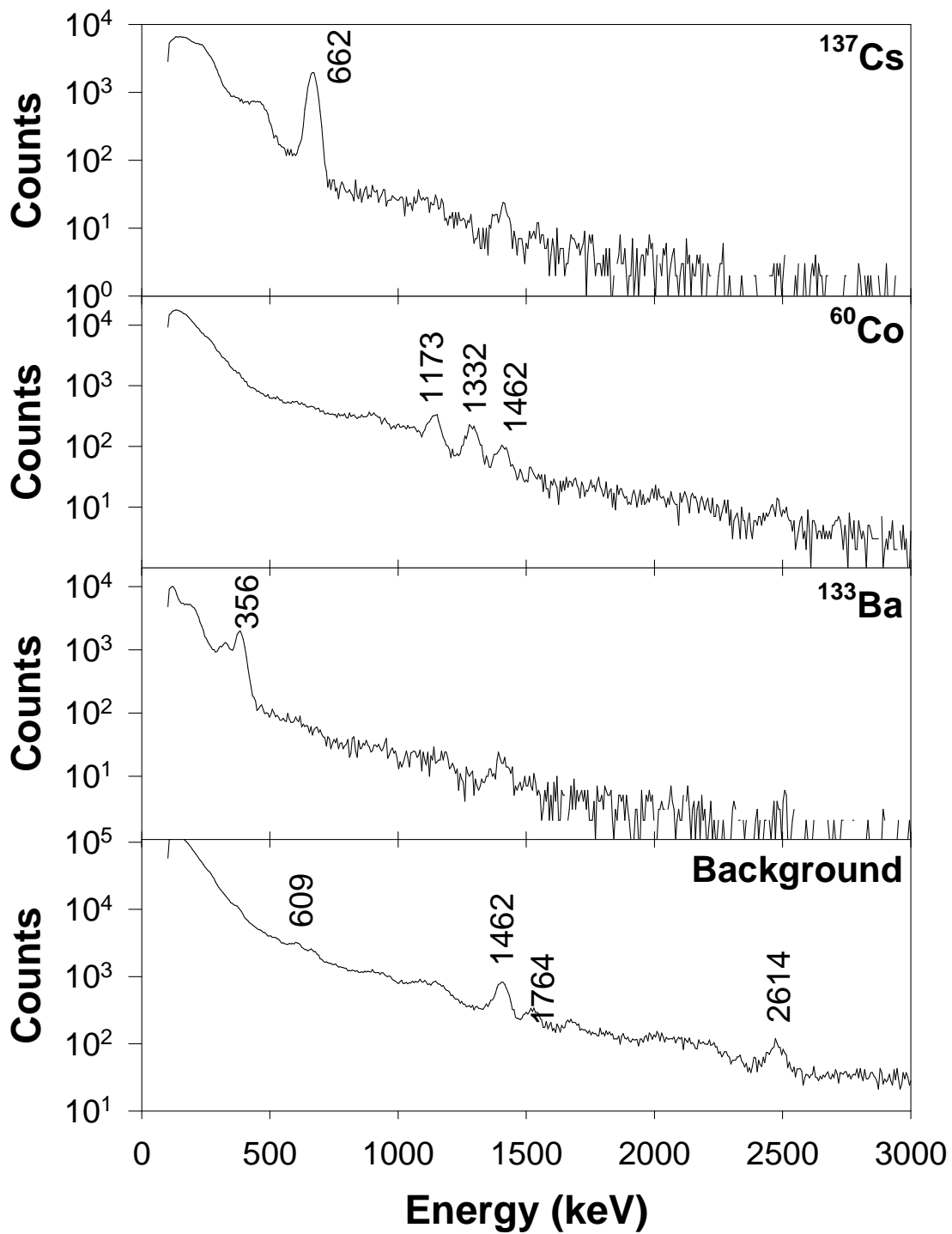


**Figure 2.7:** Spectra recorded from  $^{137}\text{Cs}$  (10000s livetime),  $^{60}\text{Co}$  (50000s livetime),  $^{133}\text{Ba}$  (10000s livetime) sources and laboratory background (400000s livetime) for the eV detector oriented horizontally.

Voltage (V)	20	40	60	70	80	100
Resolution (FWHM)	7.3%	7.1%	6.9%	7.5%*	7.3%	7.4%

\* The spectrum at 70V was recorded last, and the diode appears to have been adversely affected by operating at the maximum stated voltage.

**Table 2.2:** Resolution of the CsI(Tl) photodiode detector as a function of reverse bias voltage.

To evaluate the performance of the Hamamatsu and Canberra preamplifiers a  $^{137}\text{Cs}$  source was placed close to the detector, and the two preamplifiers used in turn to generate signals for amplification by an Ortec 570 spectroscopy amplifier with spectra recorded using a 916 ACE card. The final stage gain and ADC LLD were kept constant. Figure 2.8 shows spectra recorded using each of these preamplifiers. It is clear that the performance of the Hamamatsu unit is very poor in comparison with the Canberra and eV preamplifiers; partly due to the low inherent gain which results in a significant noise component at similar energies to the signals of interest. On the basis of these tests it was decided that the Hamamatsu preamplifier is unsuitable to the requirements of this application, which needs a system with higher gain and less noise.

The Canberra preamplifier, on the other hand, has good performance, with reasonable gain and low noise resulting in spectral characteristics comparable to the eV detector. This confirms that the crystal and diode used for the evaluation of these preamplifiers is well manufactured, and suitable for the purpose it was produced for. The size of the Canberra 970 preamplifier makes it unsuitable for use in a large array. It is, however, suitable for use with a single detector in laboratory measurements, and has been used for further work during this project, specifically a comparison of different detector sizes.

It would be possible to produce a large array of detectors using the eV preamplifier, or a similar device, however the electronics required to log spectra from such an array would be fairly complex. Such hybrid preamplifiers have fixed gain, so to produce high resolution summed spectra an additional amplifier to adjust the gain of each channel would be required. Alternatively, spectra from each element could be recorded separately, and gain matched in software. A pulse processing system similar to that envisaged for recording spectra from individual NaI(Tl) detectors could be used for an array of CsI(Tl)-photodiode detectors, however this would become increasingly more complex as the number of elements increases and would become impractical for more than about 16 elements.

An additional amplifier chip was also tested, a gamma camera IC produced by the Rutherford Appleton Laboratory (RAL). This chip, RAL-213 [44,45], is a charge amplifier and readout IC originally designed for medical imaging using Cadmium Telluride (CdTe) crystals in a continuous array of 3×3 mm crystals, and is based on the SR1 chip designed for use with CsI(Tl) photodiode detectors and used with HgI detectors for a satellite instrument [46]. This is a 16 channel chip, each channel consisting of a preamplifier, threshold comparator, variable shaping time shaping amplifier and peak hold circuit. The channel outputs are multiplexed through a single differential output, with the channel address presented simultaneously with the

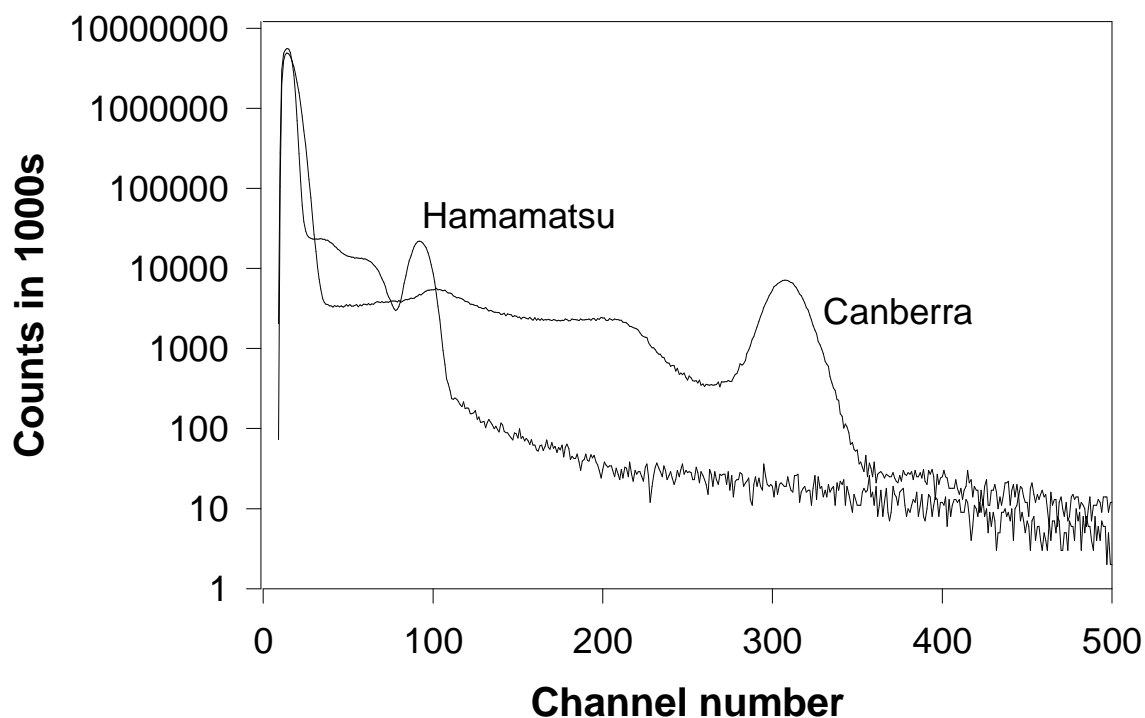


**Figure 2.8:** Spectra recorded from a  $^{137}\text{Cs}$  source using Hamamatsu H4083 and Canberra 970 pre-amplifiers.

data. Sixteen of these chips can be daisy-chained, sharing common busses, to allow 256 channels sharing a common ADC and sequence generating circuitry. The compact size and multichannel nature of these chips would be ideal for use with an array of a large number of individual CsI(Tl) crystals, if the performance of the chip is adequate.

The RAL-213 chip is controlled by a series of square pulses to initiate data collection and readout. An 8255 i/o card was used to generate these pulses, under control of a computer program. Synchronising the output of the chip with an ACE card would be extremely complex, so it was decided to use a separate ADC to generate a digital output to be read by the 8255 card. A circuit to connect the RAL-213 chip, the ADC and the i/o card was designed, and a printed circuit board produced.

The chip was provided mounted on a printed circuit board with 16 input pins on a 3 mm pitch (to match the crystal size used for biomedical imaging), each of which has a load resistor premounted. There is a 23 pin connector on the base of the board, on a 1.27 mm (0.05") pitch, to plug into a motherboard. The components, including de-coupling capacitors and control lines are mounted on a grounded backplane. A set of lines on the board are cut in order to set the chip address and shaping time. During initial evaluation of this chip none of these lines was cut, resulting in setting chip address to 1 and the shaping time to 1  $\mu\text{s}$ . Depending on which lines are cut, shaping times of 1, 2, 4 or 7  $\mu\text{s}$  are possible. Once it had been shown that the circuit worked, the relevant lines would be cut to set a 7  $\mu\text{s}$  shaping time. The 23 pin connector includes connections for the chip power supply (+5 V), comparator threshold, control signals and outputs (consisting of analogue voltage levels and digital chip and channel addresses). The analogue output from the chip is a square pulse negative relative to a nominal 3.5 V reference

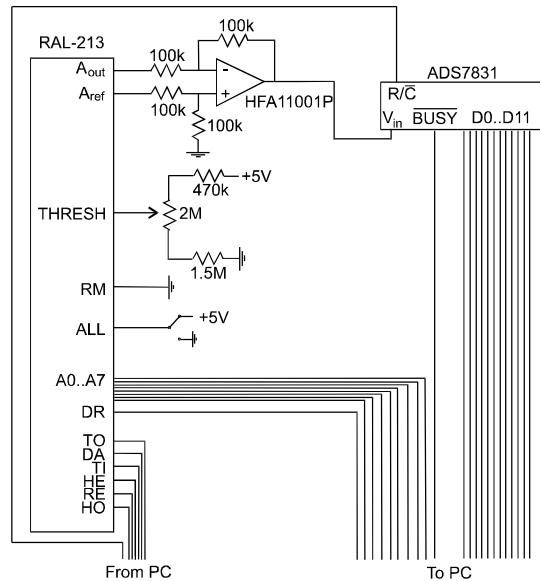


**Figure 2.9:** Schematic of the circuit used to collect data from a CsI(Tl)-photodiode detector using the RAL-213 chip and ADS7831 ADC. The positions of the lines do not reflect the actual pin positions on the chips.

voltage, which is variable between chips and may be dependent on temperature. A difference amplifier was used to produce a positive going signal relative to ground that would be independent of such factors, this required the use of a high slew rate amplifier (HFA11001P, with a  $2300 \text{ V}/\mu\text{s}$  slew rate) because of the relatively narrow output pulses.

After examination of the technical data on a variety of ADC chips an ADS7831 chip produced by Burr-Brown [42] was chosen as the best choice for the current application; this is a 12 bit successive approximation (SAR) device with inbuilt sample-and-hold circuitry, reference and clock, it has a maximum acquire and convert time of  $1.66 \mu\text{s}$  and latched two's complement binary output. The PCB made for use with the RAL-213 chip includes a potentiometer to adjust the comparator threshold, the fast difference amplifier as well as sockets for the RAL IC, the ADC and power and control line inputs. The operation of the ADC was confirmed by recording spectra from a NaI(Tl) detector, as reported in section 2.1. Figure 2.9 shows a schematic of the circuit employed. The readout mode (RM) was set to zero, resulting in a periodic readout cycle, where the detector is active for a set period of time before read-out, rather than reacting to the detection of an event. A switch was included to allow a selection between reading all the channels (ALL=1) and reading only those channels in which an event had been detected (ALL=0).

A program was written to generate the control signals for the RAL chip and the ADC, and to record the digital outputs from the ADC. For simplicity ALL was always set to one, this results in no requirement to read the channel address lines (A4 to A7), and with RM=0 the DR line is also not checked. Figure 2.10 shows the sequence of control signals for the RAL chip and ADC. At the start of each cycle the comparator is reset; hit enable (HE) is high as a result of the end of the previous cycle, the hold (HO) and reset (RE) lines are put high for  $3 \mu\text{s}$  and  $20 \mu\text{s}$  respectively,  $1 \mu\text{s}$  after RE goes low HE is also set low to enable event detection. HE is kept low for a set period ( $4 \text{ ms}$ ) and then set high to initiate readout. After HE is set high, HO is also

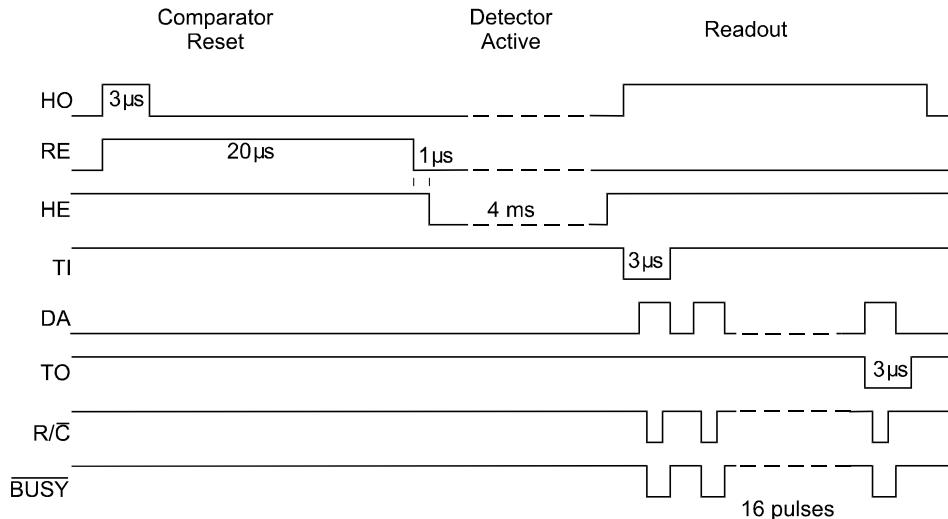


**Figure 2.10:** The sequence of control signals used to operate the RAL 213 chip and ADS7831 ADC. All signals, except  $\overline{\text{BUSY}}$  which is generated by the ADC, are produced using an 8255 interface card.

set high and token in (TI) is set low 1  $\mu\text{s}$  later, TI is held low for 3  $\mu\text{s}$  before going high. Sixteen data acquisition (DA) pulses initiate the readout of each of the 16 channels in turn. Shortly after the analogue output from each channel is presented a convert pulse ( $\text{R}/\overline{\text{C}}$  sent low for a minimum of 40 ns) is sent to the ADC, and when conversion is complete ( $\overline{\text{BUSY}}$  going high) the digital output is read. The next DA pulse is sent after the data has been read. The token out (TO) line is set low for 3  $\mu\text{s}$  at the start of the last DA pulse, and HO is set low when TO returns high. HE is kept high prior to the comparator reset.

Within the time available it proved to be difficult to overcome practical problems in getting this system to operate in a consistent and reproducible manner. There are several possible causes for these problems, mostly relating to the extremely high sensitivity of the charge inputs to the chip, and the resulting requirement for an extremely stable electrical environment. Further work would be needed to overcome the practical problems associated with the use of this circuit.

It is expected that an electronics system for operating a large environmental array will need to be able to deal with multi-detector partial energy deposition events, and as such will require an event management system of the type envisaged for the RAL-213 device. However, for the purpose of developing an experimental array to investigate the response of a multi-detector system, and to validate Monte Carlo simulations, a simpler pulse height analysis system and gating arrangement will suffice. For this purpose, a 16 channel NIM based system has been procured although a significant amount of work is still required until such an array can be produced.

### 2.3 Investigation of Crystal Dimensions.

A series of CsI(Tl) crystals of a range of sizes was ordered from Hilger Crystals in order to assess the effect of different dimensions on the performance of CsI-PIN photodiode detectors. An S3590-08 photodiode with the Canberra pre-amplifier, an Ortec 571 shaping amplifier and 916 ACE card was used to evaluate these crystals. The same diode was used throughout, and



the amplifier gain, bias voltage and ADC LLD were not adjusted during the experiment, the crystal used was the only variable. A BNC socket was attached to a large die-cast box which could be sealed to prevent light entering, and the diode connected to the inside of this socket by leads long enough to allow the diode to be attached to all the crystals when placed in the centre of the box. The diode was attached to each crystal using silicone grease to ensure good optical coupling and held in place with adhesive tape. The box was closed, and spectra were recorded from a  $^{137}\text{Cs}$  source placed 30 cm from the side of the box along and perpendicular to the axis of the crystal.

At present, only a few of these crystals have been received and tested. The crystals with diameters larger than 10 mm were tapered to a 10×10 mm square area onto which the diode was affixed, the tapering angle was approximately 45°. Table 2.3 lists the response characteristics of the crystals tested, for sources placed parallel and perpendicular to the crystal axis. There is a clear relationship between crystal dimensions and detector response. The detector gain and resolution degrades with increasing crystal size. This is the result of absorption of scintillation photons within the crystal, which is worse for large crystals in which the average photon path is much longer. The full energy peak efficiency increases with the length of crystal material along the source-detector axis, reaching a maximum efficiency with 8 cm of material along this axis. This is due to the penetration depth of 662 keV  $\gamma$ -rays in CsI(Tl), which clearly is of the order of a few cm, and also agrees with the observation that the efficiency of the eV detector was higher with the long axis aligned to the source-detector axis.

These crystals supplied by Hilger have a pink tint, which would presumably affect the light transmission within the crystals. This could be a contributing factor to the low light collection efficiency observed with the larger crystals. This discolouration had been noticed in crystals during a visit to Hilger, and ICPMS analysis conducted on these crystals. This analysis has shown that both clear and coloured crystals contain Ni impurities at between 130 and 200 ppm, although the analysis is insensitive to Fe it is assumed that it is also present. The most likely source of these contaminants is diffusion from furnace windings in the crucible into the melt. It is possible that the pink colour is due to variation in oxidation state or coordination site of these contaminants. It was also noted that the pink crystals had slightly higher Ni levels, and reduced Tl levels, implying that the Ni possibly inhibits Tl uptake in the crystal.

Diameter (mm)	Length (mm)	Source along axis			Source parallel to axis		
		Peak channel	FWHM	Efficiency	Peak channel	FWHM	Efficiency
10	50	410.2	7.6%	15.2%	412.1	6.6%	3.3%
25.4	50.8	200.9	12.0%	18.9%	193.3	11.4%	10.9%
20	85	202.2	11.8%	25.1%	204.0	11.5%	8.3%
50	120	47.0	32%	24.8%	51.4	31%	14.6%

**Table 2.3:** Peak channel, FWHM and full energy peak efficiency (after accounting for geometrical effects) for detection of  $\gamma$ -rays from a  $^{137}\text{Cs}$  source placed 30cm from the detector box along and perpendicular to the crystal axis.

### 3. Monte Carlo Simulations of CsI(Tl) Detectors.

Three generations of Monte Carlo codes have been previously developed for modelling the response of NaI(Tl) detectors [47-49]. The first of these (MCI) [47,48] is a full analogue code, and is best suited to close coupled systems where the source-detector distance is short. This code was validated for such systems. A statistical approximation approach (MCII) [47,48] was used to increase simulation speeds, and has been used for airborne geometries. This has been validated against the MCI code. To further increase simulation speed an inverse geometry approach has also been used (MCIII) [49].

In order for these Monte Carlo codes to simulate spectra for particular detectors the characteristics of the detector, specifically the variation of FWHM with energy have to be determined experimentally. These codes cannot, therefore, be used to investigate the effects of crystal size on the detector resolution without first conducting measurements on a crystal of that size. However, for crystals with known characteristics, the response of such crystals in a large array to different sources or source geometries can be simulated. Even without the prior knowledge of the spectral resolution these codes can still effectively model effects such as full energy peak efficiencies, peak to Compton ratios and self-collimation effects. Other codes, such as GEANT [50], should be capable of modelling the response of individual crystals more completely. Such codes are, however, less suited to simulating airborne geometries due to the large source to detector distances.

#### 3.1 Simulation of eV Detector Response.

The first of these codes, MCI, has been modified to simulate a CsI(Tl) detector for close-coupled source-detector geometries by replacing the NaI scattering and absorption terms with the corresponding terms for CsI. These parameters were determined using photon cross sections from Nuclear Data Tables [51]. The code was tested by simulating spectra for a 10×10×20 mm CsI(Tl) crystal in the same geometries as the eV detector previously tested.

Figure 3.1 shows the simulated and measured spectra (after subtraction of the background) for  $^{137}\text{Cs}$ ,  $^{60}\text{Co}$  and  $^{133}\text{Ba}$  with the detector aligned vertically. It can be seen that the agreement for  $^{137}\text{Cs}$  and  $^{60}\text{Co}$  is very good, however in the  $^{133}\text{Ba}$  spectrum the simulation has significantly worse resolution at low energy, which is probably a result of difficulties in determining the FWHM of peaks at these energies due to the substantial scattered component. The measured spectra also includes a large scattered peak at low energies, which is probably due to additional scatter in the laboratory that is not modelled in the Monte Carlo code which only considers scatter from a plane concrete floor, in the air path and within the crystal.

Overall the modifications made to MCI to simulate CsI(Tl) rather than NaI(Tl) scintillators have produced a code that generate reasonably accurate simulated spectra for close-coupled geometries. The same modifications have also been made to versions of MCII and MCIII to facilitate the simulation of the response of CsI(Tl) detectors in airborne geometries.

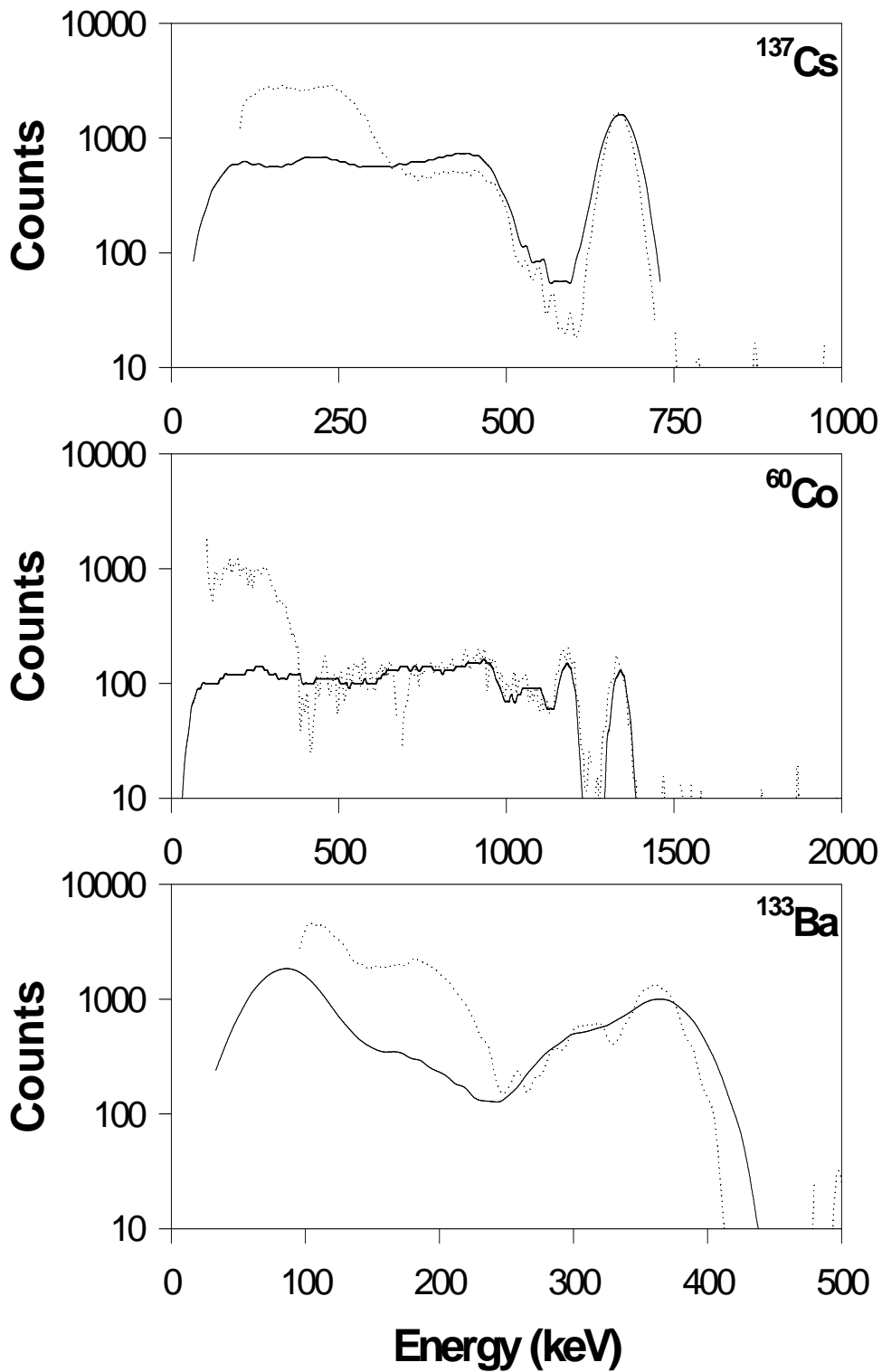


**Figure 3.1:** Comparison between experimental (dashed line) and simulated spectra for a 10x10x20 mm Cs(Tl) crystal for  $^{137}\text{Cs}$ ,  $^{60}\text{Co}$  and  $^{133}\text{Ba}$ .

Material	Energy (keV)	Full energy deposition	Number of interactions	1 <sup>st</sup> & 2 <sup>nd</sup> interaction separation (mm)
NaI(Tl)	662	78.2%	2.72±1.22	117±76
	1462	57.5%	3.20±1.28	124±79
	2614	41.3%	3.45±1.32	122±81
CsI(Tl)	662	83.1%	2.72±1.20	116±81
	1462	66.5%	3.31±1.27	129±87
	2614	52.0%	3.55±1.29	131±89

**Table 3.1:** Results from analysis of deposition lists for 662keV, 1462keV and 2614keV  $\gamma$ -rays incident on 16 litres of NaI(Tl) or CsI(Tl).

### 3.2 Analysis of Deposition Patterns Within Crystals.

The MCI codes, for both CsI(Tl) and NaI(Tl), were also modified to produce interaction lists consisting of the position and deposited energy for each interaction (up to a maximum of seven interactions per  $\gamma$ -ray) in the detector volume. The data from these codes can be used to investigate the effect of detector segmentation, and to help determine optimal dimensions for individual elements of a large array. They can also be used to investigate whether knowledge of the location of interactions within an array could provide information additional to the total energy deposited in the array, which could, for example, be used to determine the source burial depth. These interaction lists were written to files for analysis by additional programs at a later date. These secondary programs were used to generate data such as the number of incident  $\gamma$ -rays that deposited their full energy in the crystal, the number of interactions required to deposit this energy and the distances between successive interactions.

Deposition lists for one million interacting  $\gamma$ -rays in 16 litres (40.64×40.64×10.16 cm) of NaI(Tl) or CsI(Tl) crystal for sources of 662 keV, 1462 keV and 2614 keV  $\gamma$ -rays placed 1 m from the detector were generated. Table 3.1 gives the percentage of full energy events, and the weighted average number of interactions and distance between the first and second interactions for these three  $\gamma$ -ray energies in CsI(Tl) and NaI(Tl). The simulated full energy peak efficiency for the NaI(Tl) crystal is slightly larger than that which is experimentally measured (approximately 66% for <sup>137</sup>Cs). As would be expected, as a result of the greater density of CsI(Tl), a greater number of incident  $\gamma$ -rays deposit their full energy within the fixed volume of crystal. It is also not surprising that higher energy  $\gamma$ -rays are less likely to deposit their full energy in the crystal, and require more interactions to deposit their energy with a slightly greater distance between interactions. The distance between interactions is somewhat surprising given the data from the comparison between crystals of different dimensions, in which the full energy peak efficiency for <sup>137</sup>Cs  $\gamma$ -rays does not increase significantly as the length of material along the detector-source axis increases beyond about 8 cm, which implies an interaction length much less than the 11-13 cm given by this simulation. On the basis of this simulation, if individual crystals of an array had dimensions of approximately 10 cm or less then most interactions would occur in adjacent elements. The measured response of real

detectors has shown that the spectral response of crystals of this size will probably be inadequate for producing an array with comparable, or enhanced, resolution compared to NaI(Tl). Thus, it is clear that in any array produced most of the  $\gamma$ -ray interactions will be multi-detector events; and any electronics system developed for such an array would have to be able to treat such events.

A program was also written to analyse these deposition lists to produce spectra of the energy deposited in particular smaller volumes within the crystal. These should be the spectra that would be recorded from a real array of small crystal elements, although ignoring the effects of the cans and diodes surrounding each element. The production of such an array, or even a single crystal and photodiode detector within a larger volume of material, would be needed to validate the Monte Carlo codes produced here. This has yet to be done.

### 3.3 Analysis of Deposition Lists for Source Burial Analysis.

In order to investigate whether self-collimation effects within an array can provide information on source burial the MCIII codes for CsI(Tl) and NaI(Tl) were modified to produce deposition lists and to incorporate source burial. The MCIII code uses an inverted geometry to increase simulation speed, in which a virtual array of elements simulates the effect of a very large detector, a geometric correction is then applied to the resulting simulated data to produce simulated spectra for a single detector. To produce deposition lists each interaction within the virtual detector was transformed to the equivalent position within a real detector volume.

The simulation codes were run for 50000 interacting  $\gamma$ -rays in the crystal for a  $^{137}\text{Cs}$  planar source on the surface and at burial depths of 10, 20 and 30 cm with a 16 litre detector 50 m above the surface. To confirm that the code correctly accounted for the geometric differences between the real detector and the virtual array a single simulation using MCI modified for source burial was used to produce deposition lists for a NaI(Tl) detector and 10 cm source burial for 1000 interacting  $\gamma$ -rays.

Figure 3.2 shows a comparison of the total spectra for the two simulations with the modified MCI and MCIII codes for 10 cm source burial and a NaI(Tl) detector. There is clearly a big difference between the two spectra, with the MCI spectrum having significantly less scattered

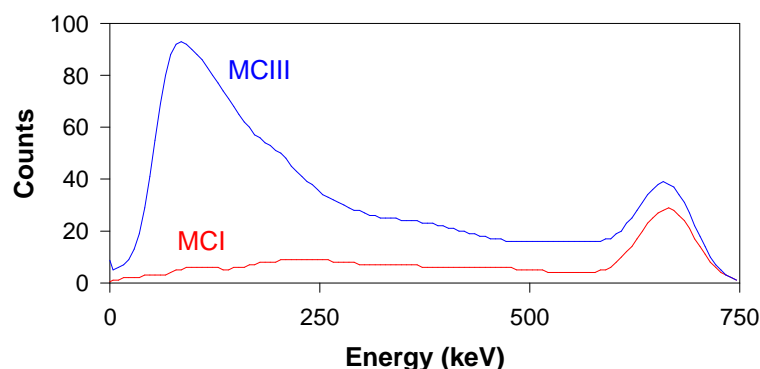


**Figure 3.2:** Comparison between simulated spectra for a planar  $^{137}\text{Cs}$  source buried under 10cm of soil with a 16 litre NaI(Tl) detector 50m above the surface using modified versions of the MCI and MCIII codes.

component. The MCIII result is the more physically believable of the two; but it is not clear why there is so little scatter in the spectra produced using MCI.

Whereas the MCI and MCII codes have been extensively validated for NaI detectors [47,48], and the MCIII code cross checked against these codes [49], a number of changes were made to MCI and MCIII to match these codes to CsI(Tl)-photodiode detectors and to analyse the interaction positions within a large detector. As noted above, the spatial distribution of energy deposition predicted by these analyses was surprisingly dispersed and spectra derived from the deposition lists for MCI show a physically unrealistic lack of scatter. Therefore, the results of these codes should be treated with caution at this stage. More work is needed to validate these codes further and to compare them with other MC simulations of sources in laboratory geometries, and with experimental results from a small array of detectors.

#### 4. Discussion and Conclusions.

Airborne Gamma Spectrometry (AGS) is a well recognised method of measuring the distribution of radioisotopes in the environment. Conventionally, AGS systems consist of a number of large volume NaI(Tl) crystals coupled to bi-alkali photomultipliers, with a resolution of 9-10% FWHM for the 662 keV  $^{137}\text{Cs}$   $\gamma$ -ray for the combined array. For several isotopes of interest in environmental research the associated  $\gamma$ -rays may be difficult to resolve, and the resolution of airborne systems can be a limiting factor in measuring the activity of such isotopes. Some methods of improving the performance of AGS detector systems have been investigated, specifically improvements to the electronics for NaI(Tl) detectors and the possibility of using CsI(Tl) crystals coupled to Si PIN photodiodes.

It has been demonstrated that the performance of NaI(Tl) detectors can be improved by using a more sophisticated shaping amplifier, consisting of a differentiation and two integration stages. This amplifier improves the resolution of one NaI(Tl) detector from 9.0% FWHM for  $^{137}\text{Cs}$   $\gamma$ -rays to 8.2%, without the benefit of having the amplifier in a shielded box. Using this shaping amplifier instead of the summing amplifier currently used would be a simple modification to the AGS system that would result in improved spectral resolution.

Some possible methods for combining this improved amplifier with a discrete SAR ADC chip have been considered. These would enable more flexible approaches to data collection and processing than simply recording the total energy deposited in the entire array. This could include recording spectra from individual crystals or from the inner and outer pairs; these systems have yet to be experimentally investigated. Such flexible data processing could allow self-collimation and angular correlation effects within the array to be exploited to gain additional information on source distribution and burial that could enable more accurate calibration of airborne equipment.

The properties of CsI(Tl) crystals, when combined with Si PIN photodiodes, are suitable for the production of a detector system which combines high intrinsic efficiency with improved resolution compared to NaI(Tl) crystals coupled to photomultipliers. Such detectors also eliminate the requirement for high voltage supplies, and would be less bulky than NaI(Tl) detectors of equivalent efficiency. However, the high capacitance of photodiodes limits their size to a few  $\text{cm}^2$ , resulting in the use of smaller crystals than those which can be used for NaI(Tl) detectors.

The possibility of using CsI(Tl) coupled to photodiodes for AGS instead of large volume NaI(Tl) detectors has been investigated. To produce a detector system with sufficient efficiency for such applications an array containing a large number, possibly as many as 256, of smaller crystals would be needed. It is expected that self-collimation and angular distribution effects within such an array would be better defined than with a conventional NaI(Tl) array of four crystals due to the larger number of elements.

A variety of CsI(Tl)-PIN photodiode detector systems have been examined with the view of developing such an array of detectors for use in AGS or other radiometric systems. A single commercially available detector, produced by eV Products, comprising a  $10 \times 10 \times 20$  mm CsI(Tl) crystal with a  $10 \times 10$  mm photodiode and hybrid preamplifier has been tested. A test detector, consisting of a  $14 \times 14 \times 20$  mm CsI(Tl) crystal mounted on a Hamamatsu S3590-08

photodiode was produced to evaluate other separate preamplifiers and associated electronics. A small range of different crystal sizes was also tested to help optimise crystal dimensions. Some Monte Carlo simulation codes have also been developed, although some of the outputs of these codes produce results which are not entirely believable, and are treated with caution at this stage.

The eV detector has a maximum resolution of 6.0% and full energy peak efficiency of 9.7% for  $^{137}\text{Cs}$   $\gamma$ -rays, depending on electronics and detector orientation, with a low energy threshold of approximately 100 keV. This has confirmed the improved spectral resolution of small CsI(Tl) crystals coupled to photodiodes. However, crystals of this size may be considered undesirably inefficient for use in an airborne detector. If larger crystals can approach the performance of this crystal then a large detector array is more feasible.

A H4083 discrete compact preamplifier manufactured by Hamamatsu Photonics and designed to work with the S3590 series of photodiodes for direct conversion of radiation in the diode was evaluated for use with a CsI(Tl)-photodiode detector. It was shown that the gain on this amplifier is too low for the requirements for this project, having the peak due to  $^{137}\text{Cs}$  within the amplifiers electronic noise. No further testing with this amplifier was conducted.

An old Canberra 970 preamplifier, borrowed from the Glasgow University Physics Department, containing a number of discrete components within a fairly large box, was also evaluated. This had good noise and gain characteristics, confirming that the test detector had been manufactured to a quality similar to the eV device. This amplifier has been used for laboratory tests of a range of different crystal sizes, although its size makes it unsuitable for use in a large array.

Variations on the proposed electronics for recording spectra from individual NaI(Tl) detectors could be used with discrete preamplifiers such as the eV hybrid chip in an array of several CsI(Tl)-photodiode detectors. However, such a data logging system would become very complex with larger arrays, and would probably be limited to arrays of approximately 16 elements. The RAL-213 gamma camera IC, based on the SR1 chip, is a 16 channel device with each channel consisting of a preamplifier, threshold comparator, variable shaping time shaping amplifier and peak hold circuit. Sixteen of these chips can be daisy-chained, sharing common busses, to allow 256 channels sharing a common ADC and sequence generating circuitry. The compact size and multichannel nature of these chips would be ideal for use with an array of a large number of individual CsI(Tl) crystals, if the performance of the chip is adequate.

A circuit was developed to use the RAL-213 chip in conjunction with a Burr-Brown ADS7831 SAR ADC chip using an 8255 i/o board and a simple program to manage spectral logging. The analogue output from the chip is a square pulse negative relative to a nominal 3.5 V reference voltage, and is variable between chips and may be temperature dependent. A high slew rate difference amplifier was used to produce a positive going signal relative to ground that would be independent of such factors. Within the time available it proved to be difficult to overcome practical problems getting this system to operate in a consistent and reproducible manner. There are several possible causes for these problems, mostly relating to the extremely high sensitivity of the charge inputs to the chip and the resulting requirements for an extremely stable electrical environment. Further work would be needed to overcome the practical problems associated with the use of this circuit. However, when these problems are overcome



this circuit and a slightly modified version of the code would readily log spectra from a 16 element array and modifications to this system to log spectra from several such 16 channel systems would be relatively straight forward.

It has been shown that CsI(Tl)-PIN photodiode detectors can produce spectra with higher resolution than conventional NaI(Tl)-photomultiplier detectors, however for use in a large array for AGS it would be more practical to use larger crystals. To determine if larger crystals have sufficiently good spectral responses, and to aid the optimisation of crystal dimensions, the characteristics of a number of crystals of different sizes has also been conducted, keeping the photodiode and amplification constant. This has shown that it is possible to maintain good spectral resolution for crystal larger than the few cm<sup>3</sup> that have been used previously, although the gain and resolution degrades with increasing crystal size as a result of absorption of scintillation photons within the crystal, which is worse for large crystals in which the average photon path is much longer. The full energy peak efficiency increases with the length of crystal material along the source-detector axis, reaching a maximum efficiency with about 8 cm of material along this axis. This is due to the penetration depth of 662 keV  $\gamma$ -rays in CsI(Tl), which clearly is of the order of a few cm.

The crystals tested, when mounted, have a pink tint, which is expected to effect the transmission of scintillation luminescence within the crystals, and thus explain the low light collection efficiency of the larger crystals. Similar discolouration had been noticed in crystals during a visit to Hilger, and ICPMS analysis conducted on samples. This has shown that both clear and coloured crystals contain Ni impurities at between 130 and 200 ppm; it is assumed that Fe is also present although the analysis is insensitive to it. The most likely source of these contaminants is diffusion from furnace windings in the crucible into the melt. It is possible that the pink colour is due to variation in oxidation state or coordination site of these contaminants. It was also noted that the pink crystals had slightly higher Ni levels, and reduced Tl levels, implying that the Ni may inhibit Tl uptake in the crystal.

Further work is still required to determine optimal crystal size and tapering angle, and the potential for improving crystal transparency and luminescence efficiency. All of these steps are expected to add to the viability of CsI(Tl) for environmental gamma spectrometry. It is, nevertheless, apparent that a sufficiently large array of small crystals would have superior performance to NaI(Tl) detectors for the 0.2-3 MeV energy range.

Monte Carlo codes that had been previously developed to simulate NaI(Tl) AGS detector systems have been modified to simulate CsI(Tl) detectors. To fully simulate spectra these codes require experimentally measured spectral characteristics, and so cannot, therefore, be used to investigate the effects of crystal size on the detector resolution. However, for crystals with known characteristics, the response of such crystals in a large array to different sources or source geometries can be simulated. Even without the prior knowledge of the spectral resolution these codes can still effectively model effects such as full energy peak efficiencies, peak to Compton ratios and self-collimation effects. Other codes, such as GEANT, should be capable of modelling the response of individual crystals more completely but are less suited to simulating airborne geometries due to the large source to detector distances.

The simple modification of changing NaI(Tl) specific terms to the equivalent CsI(Tl) parameters has successfully modelled a small CsI(Tl)-PIN photodiode detector produced by

eV Products, in a close-coupled geometry.

The Monte Carlo codes, for both CsI(Tl) and NaI(Tl), were also modified to produce interaction lists consisting of the position and deposited energy for each interaction in the detector volume. This data can be used to investigate the effect of detector segmentation, help determine optimal dimensions for individual elements of a large array, and investigate angular correlation and self-collimation effects. The results of these simulations slightly over estimate the full energy peak efficiency for NaI(Tl), but produce the physically realistic results that full energy peak efficiency is greater for CsI(Tl) than NaI(Tl) and that higher energy  $\gamma$ -rays have lower efficiencies. The distance between interactions is somewhat surprising given the data from the comparison between crystals of different dimensions. Spectra for particular small volumes within the crystal, corresponding to elements in an array, may also be produced, although this has yet to be done.

To investigate whether self-collimation effects within an array can provide information on source burial these codes, for CsI(Tl) and NaI(Tl), were also modified to incorporate source burial. The results of these modifications, for an otherwise extensively validated code, produced spectra with a non-physically realistic lack of scatter. Because of this effect, and the surprisingly dispersed spatial distribution of energy deposition noted above, the results should be treated with caution at this stage. More work is needed to validate these codes further and to compare them with other MC simulations of sources in laboratory geometries, and with experimental results from a small array of detectors.

It has been shown that it is possible to improve on the spatial response and data acquisition systems currently used in AGS through modifications to the electronics and computational methods used with existing NaI(Tl) detectors. It has also been shown that the use of CsI(Tl) crystals coupled to Si PIN photodiodes can generate data with greater spectral resolution than NaI(Tl), although only for relatively small crystals. Although there is still considerable work to be done to produce a large volume array of CsI(Tl) detectors for use in AGS, some of the means by which such an array could be constructed and operated have been identified. These improvements should enhance the ability of AGS to quantify the activity of radioisotopes in the environment through reduced spectral interferences and better knowledge of source distribution.

## **Acknowledgements.**

The work presented here was funded by the UK Engineering and Physical Sciences Research Council (EPSRC), grant number GR/M15842. The eV detector was loaned for evaluation purposes by Gresham Scientific Instruments Ltd. Hilger Crystals Ltd supplied several CsI(Tl) crystals for evaluation trials, and constructive discussions with Jim Telfer and George Smith were held. The Canberra 970 preamplifier was borrowed from the Department of Physics and Astronomy, Glasgow University. Marcus French and Steve Thomas of the Rutherford Appleton Laboratory Microelectronics group kindly provided several RAL-213 units for evaluation, and Steve Thomas provided considerable assistance in trying to get them to operate successfully. ICPMS studies of samples of CsI(Tl) crystals were conducted at SURRC by Dr. McCartney.

## References.

- [1] D.C.W. Sanderson, E.M. Scott, M.S. Baxter, *Use of airborne radiometric measurements for monitoring environmental radioactive contamination, Environmental Contamination Following a Major Nuclear Accident*. Proceedings of a Symposium. IAEA-SM-306/138, Vol. 1, 411-421 (1990).
- [2] D.C.W. Sanderson, J.D. Allyson, A.N. Tyler, E.M. Scott, *Environmental applications of airborne gamma spectrometry*, IAEA Technical Committee Meeting on the Use of Uranium Exploration Data and Techniques in Environmental Studies. Proceedings of a Technical Committee meeting held in Vienna, 9-12 November 1993. IAEA-TECDOC-827, 71-91 (1995).
- [3] D.C.W. Sanderson, J.D. Allyson, A.N. Tyler, *Rapid quantification and mapping of radiometric data for anthropogenic and technologically enhanced natural nuclides*, IAEA Technical Committee Meeting on the Use of Uranium Exploration Data and Techniques in Environmental Studies. Proceedings of a Technical Committee meeting held in Vienna, 9-12 November 1993. IAEA-TECDOC-827, 197-216 (1995).
- [4] *Airborne Gamma Ray Spectrometer Surveying*, Technical Report Series No. 323, International Atomic Energy Agency (1991).
- [5] *Gamma-ray Spectrometry in the Environment*, International Commission on Radiation Units and Measurements Report 53 (1994).
- [6] D.C.W. Sanderson, J.M. Ferguson, *The European capability for environmental airborne gamma ray spectrometry*, Radiat. Prot. Dosim. **73(1-4)**, 213-218 (1997).
- [7] D.C.W. Sanderson, J.D. Allyson, K.J. Cairns, P.A. MacDonald, *A Brief Aerial Survey in the Vicinity of Sellafield in September 1990*, SURRC report (1990).
- [8] D.C.W. Sanderson, J.D. Allyson, A.N. Tyler, *An Aerial Gamma Ray Survey of Chapelcross and its Surroundings in February 1999*, SURRC report (1992).
- [9] D.C.W. Sanderson, J.D. Allyson, A.N. Tyler, *An Aerial Gamma Ray Survey of Springfields and the Ribble Estuary in September 1992*, SURRC report (1993).
- [10] D.C.W. Sanderson, J.D. Allyson, S. Ni Riain, G. Gordon, S. Murphy, S. Fisk, *An Aerial Gamma Ray Survey of Torness Nuclear Power Station 27-30 March 1994*, SURRC report (1994).
- [11] D.C.W. Sanderson, J.D. Allyson, G. Gordon, S. Murphy, A.N. Tyler, S. Fisk, *An Aerial Gamma Ray Survey of Hunterston Nuclear Power Station on 14-15th April and 4th May 1994*, SURRC report (1994).
- [12] D.C.W. Sanderson, J.D. Allyson, S. Murphy, P. McConville, *An Aerial Survey of the Surrounding Area of the HM Naval Base Clyde*, SURRC report (1996).
- [13] D.C.W. Sanderson, J.D. Allyson, A.J. Cresswell, *An Aerial Gamma Ray Survey of the Surrounding Area of Sizewell Nuclear Power Station*, SURRC report, IMC ref: RP/GNSR/5031 (1997).

- [14] D.C.W. Sanderson, E.M. Scott, M.S. Baxter, E. Martin, S. Ni Riain, *The Use of Aerial Radiometrics for Epidemiological Studies of Leukaemia*, SURRC report (1993).
- [15] D.C.W. Sanderson, E.M. Scott, *An Aerial Radiometric Survey in West Cumbria in 1988*, MAFF Food Science Report N611 (1989).
- [16] D.C.W. Sanderson, B.W. East, E.M. Scott, *Aerial Radiometric Survey of Parts of North Wales in July 1989*, SURRC report (1989).
- [17] D.C.W. Sanderson, J.D. Allyson, E. Martin, A.N. Tyler, E.M. Scott, *An Aerial Gamma-ray Survey of Three Ayrshire Districts*, Commissioned by the District Councils of Cunninghame, Kilmarnock and Loudoun, and Kyle and Carrick, SURRC report (1990).
- [18] D.C.W. Sanderson, J.D. Allyson, A.N. Tyler, S. Ni Riain, S. Murphy, *An Airborne Gamma Survey of Parts of SW Scotland*, SURRC report (1994).
- [19] D.C.W. Sanderson, J.D. Allyson, P. McConville, S. Murphy, J. Smith, *Airborne Gamma Ray Measurements Conducted During an International Trial in Finland*, RESUME 95: Rapid Environmental Surveying Using Mobile Equipment, NKS Final Report, 237-253 (1997).
- [20] D.C.W. Sanderson, A.J. Cresswell, J.D. Allyson, P. McConville, *Experimental Measurements and Computer Simulation of Fission Product Gamma-ray Spectra*, Commissioned by the Radioactive Substances Division, Department of the Environment, Transport and the Regions, Report No. DETR/RAS/97.002 (1997).
- [21] D.C.W. Sanderson, J.D. Allyson, A.J. Cresswell, P. McConville, *An Airborne and Vehicular Gamma Survey of Greenham Common, Newbury District and Surrounding Areas*, SURRC Final Report, commissioned by Newbury District Council and Basingstoke & Deane Borough Council (1997).
- [22] I. Winkelmann, M. Thomas, G. Carloff, *Aerial measurements of radioactivity in the environment*, Kerntechnik **62(2-3)**, 118-121 (1997).
- [23] L. Guillot, *Spectrométrie Gamma Aéroportée: Etudes de nouvelles méthodes de traitement spectral et de calibration permettant une interprétation qualitative et quantitative des mesures*, PhD Thesis, L'Université de Bourgogne (1996).
- [24] J. Hovgaard, *Airborne Gamma-ray Spectrometry, Statistical Analysis of Airborne Gamma-ray Spectra*, PhD Thesis, Technical University of Denmark (1994).
- [25] G.F. Knoll, *Radiation Detection and Measurement*, John Wiley & Sons (1989).
- [26] H. Grassman, E. Lorenz, H.-G. Moser, *Properties of CsI(Tl) - renaissance of an old scintillation material*, Nucl. Instr. and Meth. **228**, 323-326 (1985).
- [27] T. Carter, A.J. Bird, A.J. Dean, D. Ramsden, *The optimisation of CsI(Tl)-PIN photodiode detectors*. Nucl. Instr. and Meth. **A348**, 567-571 (1994).
- [28] Z. He, S.V. Guru, D.K. Wehe, G.F. Knoll, A. Truman, D. Ramsden, *Portable wide-angle  $\gamma$ -ray vision systems*, IEEE Trans. Nucl. Sci. **42(4)**, 668-674 (1995).

- [29] Z. He, J. Obermark, J. Du, D.K. Wehe, S.W. Lee, G.F. Knoll, *The CSPD-1  $\gamma$ -ray vision system*, IEEE Trans. Nucl. Sci. **43**(3), 1554-1558 (1996).
- [30] J.R.M. Annand, J.C. McGeorge, G.J. Miller, V. Holliday, L. Isaksson, *A large-solid-angle CsI(Tl) proton spectrometer*, Nucl. Instr. and Meth. **A292**, 129-134 (1990).
- [31] V. Prat, H. Simon, A. Kazandjian, R. Régál, P. Siffert, *Gamma-ray spectrometry using silicon based scintillation probes*, Nucl. Instr. and Meth. **A380**, 209-214 (1996).
- [32] Yu.G. Kudenko, O.V. Mineev, J. Imazato, *Design and performance of the readout electronics for the CsI(Tl) detector*, Nucl. Instr. and Meth. **A411**, 437-448 (1998).
- [33] F. Tonetto, U. Abbondanno, M. Chiari, P.M. Milazzo, L. Travaglini, *Optimizing performances of CsI(Tl) crystals with a photodiode readout*, Nucl. Instr. and Meth. **A420**, 181-188 (1999).
- [34] J.A. Gregel, *A Proton Detector for Medium Energy Physics*, MSc Thesis, University of Glasgow (1995).
- [35] R.J. Evans, I.D. Jupp, F. Lei, D. Ramsden, *Design of a large-area CsI(Tl) photo-diode array for explosives detection by neutron-activation gamma-ray spectroscopy*, Nucl. Instr. and Meth. **A422**, 900-905 (1999).
- [36] B.E. Patt, J.S. Iwaczyk, *Improved energy resolution for scintillator based gamma-ray detectors obtained using a CsI(Tl)/Si-PIN detector*, Rev. Sci. Instrum. **68**(10), 3926-3927 (1997).
- [37] *Si Photodiodes and Charge Sensitive Amplifiers for Scintillation Counting and High Energy Physics*, Hamamatsu Photonics product catalogue (1997).
- [38] V. Radeka, *Signal, noise and resolution in position-sensitive detectors*, IEEE Trans. Nucl. Sci. **NS-21**, 51 (1974).
- [39] A. Pernick, I. Orion, D. Ilzyer, H. Zafrir, *Applications of a self-collimating BGO detector system to radiological emergency response*, Health Physics **72**(1), 136-140.
- [40] P.A. Norreys, M. Santala, E. Clark, M. Zepf, I. Watts, F.N. Beg, K. Krushelnick, M. Tatarakis, A.E. Dangor, X. Fang, P. Graham, T. McCanny, R.P. Singhal, K.W.D. Ledingham, A. Cresswell, D.C.W. Sanderson, J. Magill, A. Machacek, J.S. Wark, R. Allot, B. Kennedy, D. Neely, *Observation of a highly directional  $\gamma$ -ray beam from ultrashort, ultraintense laser pulse interactions with solids*, Physics of Plasmas **6**(5), 2150-2156 (1999).
- [41] P. Krejčíř, *An Estimator of the Radioactivity Inventory in Solway Firth and Ribble Estuary*, PhD Thesis, Charles University Prague (1999).
- [42] *ADS7831 12-Bit 600kHz Sampling CMOS Analogue-to-Digital Converter*, Burr-Brown Corporation data sheet (1995).
- [43] *eV Products CsI(Tl)/PD Detector Information for Gresham Scientific eV-1743*, test data for detector S/N: A1771 (1998).

- [44] *RAL-213 Specification Sheet*, Rutherford Appleton Laboratory Microelectronics Group
- [45] *Instructions for the Operation of Gamma Camera Modules*, Rutherford Appleton Laboratory Microelectronics Group (1998).
- [46] M.L. Prydderch, P. Seller, *A 16-channel continuous charge amplifier with sparse readout*, Nucl. Instr. and Meth. **A380**, 361-365 (1996).
- [47] J.D. Allyson, *In-situ and Aerial Environmental Radioactivity Measurements: An Investigation of Some Factors Relating to Calibration by Simulation and Experiment*, PhD Thesis, University of Glasgow (1994).
- [48] J.D. Allyson, D.C.W. Sanderson, *Monte Carlo simulation of environmental airborne gamma-spectrometry*, Journal of Environmental Radioactivity **38(3)**, 259-282 (1998).
- [49] J.D. Allyson, D.C.W. Sanderson, A.J. Cresswell, *Extended development of a Monte Carlo code for airborne radiometric survey*, paper submitted to Journal of Environmental Radioactivity.
- [50] *GEANT 3.21*, CERN Data Handling Division (Geneva, 1994).
- [51] E. Storm, H.I. Israel, *Photon cross sections from 1 keV to 100 MeV for elements Z=1 to Z=100*, Nuclear Data Tables **A7(6)** (1970).